L. LEIBMAN

DAVID W. TAYLOR NAVAL SHIP RESEARCH AND DEVELOPMENT CENTER

Bethesda, Maryland 20084

COMPUTATION OF THE SECOND-ORDER STEADY FORCES ACTING ON A SURFACE SHIP IN AN OBLIQUE WAVE

BY

Y. H. KIM

APPROVED FOR PUBLIC RELEASE; DISTRIBUTION UNLIMITED

SHIP PERFORMANCE DEPARTMENT REPORT

March 1981

DTNSRDC/SPD 0964-01

Program - ADDRES -

SECURITY CLASSIFICATION OF THIS PAGE (When Data Entered)

REPORT DOCUMENTATION PAGE

READ INSTRUCTIONS BEFORE COMPLETING FORM

1. REPORT NUMBER	2. GOVT ACCESSION NO. / 3. RECIPIENT'S CATALOG NUMBER
4. TITLE (and Subtitle)	5. TYPE OF REPORT & PERIOD COVERED
COMPUTATION OF THE SECOND-ORDER STEADY FORCES ACTING ON A SURFACE SHIP IN AN OBLIQUE WAVE	FINAL
	6. PERFORMING ORG. REPORT NUMBER
7. AUTHOR(s)	8. CONTRACT OR GRANT NUMBER(s)
YOON-HO KIM	
9. PERFORMING ORGANIZATION NAME AND ADDRESS	10. PROGRAM ELEMENT, PROJECT, TASK AREA & WORK UNIT NUMBERS
DAVID W. TAYLOR NAVAL SHIP R&D CENTER SHIP PERFORMANCE DEPARTMENT BETHESDA, MARYLAND 20084	Program Element 61153N Project SR0230101 Work Unit 1524-680
11. CONTROLLING OFFICE NAME AND ADDRESS	12. REPORT DATE
NAVAL SEA SYSTEMS COMMAND WACHINGTON, D.C. 20362	SEPTEMBER 1980
	13. NUMBER OF PAGES 48+vii
14. MONITORING AGENCY NAME & ADDRESS (if different from Controlling Office)	15. SECURITY CLASS. (of this report) UNCLASSIFIED
	15a. DECLASSIFICATION/DOWNGRADING SCHEDULE

16. DISTRIBUTION STATEMENT (of this Report)

APPROVED FOR PUBLIC RELEASE: DISTRIBUTION UNLIMITED

17. DISTRIBUTION STATEMENT (of the abstract entered in Block 20, if different from Report)

18. SUPPLEMENTARY NOTES

19. KEY WORDS (Continue on reverse side if necessary and identify by block number)

SHIP RESISTANCE
SHIP MOTION
DIFFRACTION

20. ABSTRACT (Continue on reverse side if necessary and identify by block number)

The numerical procedure of calculating the second-order steady forces is presented. The computer program is developed on the basis of Lin and Reed's theory(1976). Ship motion and diffraction potentials are required as input data for Kochin-function calculation. In order to avoid the irregular frequencies which are associated with Frank's close-fit method(1967), a modification which extends the source distribution onto the calm waterline inside of a body is made. For the diffraction problem, instead of a Helmholtz equation,

DD FORM 1 JAN 73 1473 EDITION OF 1 NOV 65 IS OBSOLETE
S/N 0102-LF-014-6601

SECURITY CLASSIFICATION OF THIS PAGE (When Data Entered)

a two dimensional Laplace's equation is used. Numerical computation for the head-sea case shows the same trend of experimental data throughout the frequency ranges but its magnitude is much larger than that of the experiment.

TABLE OF CONTENTS

LIST OF FIGURES

LIST OF TABLES

NOTATION

A	Incident wave amplitude
B	Ship beam
F_n	Froude number, $F_n = U/(gL)^{\frac{1}{2}}$
ΔF_x	Non-dimensionalized added-resistance coefficient
ΔF_y	Non-dimensionalized lateral drift-force coefficient
$\langle F \rangle$	Time average of a function F, $\langle F \rangle = 1/T \int_0^T F(t)dt$
$\langle \Delta F \rangle$	The second-order steady force
$\langle \Delta F_1 \rangle$	Added resistance
$\langle \Delta F_2 \rangle$	Lateral drift force
$\langle \Delta F_{BB} \rangle$	The second-order force due to the ship-generated waves
$\langle \Delta F_{1BB} \rangle$	Added resistance due to the ship-generated waves
$\langle \Delta F_{2BB} \rangle$	Lateral drift force due to the ship-generated waves
$\langle \Delta F_{IB} \rangle$	The second-order force due to interactions between the incoming wave and the ship-generated waves
$\langle \Delta F_{1IB} \rangle$	Added resistance due to interaction between the incoming wave and the ship-generated waves
$\langle \Delta F_{2IB} \rangle$	Lateral drift force due to interaction between the incoming wave and the ship-generated waves
g	Gravitational acceleration
$G(P,Q)$	Green's function
$H(u,\lambda)$	Kochin function
$H_j(u,\lambda)$	Kochin function due to the j-th mode of ship motion
$H_D(u,\lambda)$	Kochin function due to the diffraction potential
k_0	Wave number of the progressive wave, $k_0 = \sigma^2/g$
L	Ship length
(n_1, n_2, n_3)	Components of unit normal vector

(N_2,N_3)	Two-dimensional components of unit normal vector in y-z plane
$Oxyz$	Coordinate system translating with speed U in the Ox direction
$P=(x,y,z)=\underset{\sim}{X}$	Field point
$\underset{\sim}{q}(x,y,z,t)$	Absolute velocity, $\underset{\sim}{q} = \nabla\Phi$
$Q=(x_0,y_0,z_0)$	Singular point, or point on a body surface
r	Distance between P and Q
S_{B0}	Mean surface of ship
U	Mean forward speed of ship
$\underset{\sim}{v}(x,y,z)$	Absolute perturbation velocity, $\underset{\sim}{v} = \nabla\phi = (u,v,w)$
β	Wave heading: $\beta = 0$ - following seas, $=\pi/2$ - beam seas, $=\pi$ - head seas.
λ	Wave length of incoming wave
ν	ω^2/g
ρ	Fluid density
σ	Incoming wave frequency
τ	$U\omega/g$
Φ	Total velocity potential, a real function
ϕ	Perturbation velocity potential, a real function $\phi = \phi_S + \phi_T = \phi_S + \phi_I + \phi_B = \phi_S + \phi_I + \phi_D + \phi_M$
ϕ_B	Body-generated velocity potential
ϕ_D	Diffraction potential due to presence of ship
ϕ_I	Incident wave potential
ϕ_M	Forced-oscillatory wave potential

NOTATION (CONTINUED)

ϕ_S	Steady-state portion of ϕ
ϕ_T	Time-dependent portion of ϕ
ψ	Perturbation potential, a complex function
ψ_B	Body-generated velocity potentail
ψ_D	Diffraction potential
ψ_I	Incoming wave potential
ψ_j	The jth mode oscillatory potential
Ψ_D	Two-dimensional diffraction potential, a complex function
ω	Frequency of encounter, $\omega = \sigma - k_0 U\cos\beta$

ABSTRACT

The numerical procedure of calculating the second-order steady forces is presented. The computer program is developed on the basis of Lin and Reed's theory(1976). Ship motion and diffraction potentials are required as input data for Kochin-function calculation. In order to avoid the irregular frequencies which are associated with Frank's close-fit method(1967), a modification which extends the source distribution onto the calm waterline inside of a body is made. For the diffraction problem, instead of a Helmholtz equation, a two-dimensional Laplace's equation is used. Numerical computation for the head-sea case shows the same trend of experimental data throughout the frequency ranges, but its magnitude is much larger than that of the experiment.

Magnitude is large than the experiment →

ADMINISTRATIVE INFORMATION

This project was authorized by the Naval Sea System Command with funding under Element 61153N Project SR0230101 and identified as Work Unit Number 1524-680.

- Added Resistance
- Lateral Drift Force

INTRODUCTION

It is a well known fact that when a ship is navigating in a seaway, the engine power must be increased by a considerable amount in order to keep the same speed of advance as in calm water. Especially for a high-speed vessel or a ship on a tight schedule, it is important to predict the additional power needed in advance not only for navigational safety but also for economical reasons. The steady force induced by waves in the beamwise direction is the lateral drift force. One may state that added resistance is important from the standpoint of powering and design, and drift force from the standpoint of seakeeping and control. Both the lateral drift force and the added resistance arise from the ship motion and diffraction of waves.

These two forces are not seemingly related to each other, but from a mathematical point of view, they can be analyzed by identical method. In what follows we shall call both added resistance and lateral drift force as the second-order steady forces. Because of the complexity of the problem, there have been only a few efforts to study the second-order steady forces analytically or experimentally in the past. The traditional practice accepted by naval architects has been that power increase in a seaway is between 15-30% of the power required for calm-water resistance.

Fortunately, the advent of large computer facilities and the rapid growth of new computational technique for predicting ship motion make it possible to calculate the second-order steady forces analytically. In the last decade much work has been devoted to solving this problem, nevertheless all the studies have remained limited in scope and achievement. In 1976 Lin and Reed presented a new approach for evaluating the second-order steady forces in oblique waves. The forces are derived from linear momentum consideration. The second-order steady forces are obtained in terms of the Kochin function $H(u,\lambda)$ by taking a time-average of the periodic forces and invoking the method of stationary phase evaluation of the potentials at a large distance from the ship. The computation of second-order steady forces will be based on the formulae derived by Lin and Reed, for their approach is not only mathematically sound but also much more versatile than any other method.

The validity of the computed results is confirmed by checking with available model-experimental and other theoretical values, and, also, the effectiveness of the computer program as an inexpensive way of obtaining useful information is ascertained. The computer program developed here may be utilized for such practical application as establishing data base for the design of a ship for a given route and sea state. The work will be presented in the order of a brief outline of the mathematical problem, description of the procedure of numerical calculation, presentation of the numerical results, and finally a summarization of the findings of the study.

REVIEW OF MATHEMATICAL FORMULATION

A brief outline of the most important aspects of the theory will be presented here. More detailed derivations can be found in the report by Lin and Reed (1976).*

The problem to be considered here is that of a ship moving at constant forward speed U with arbitrary heading in a plane of progressive waves, as illustrated in Figure 1. Main assumptions and restrictions in the theory are listed below:

(1) The usualy ideal-fluid assumption is made, permitting the use of potential-flow theory;

(2) The ship has small displacement from the equilibrium position and both the incoming waves and those created by the ship are small;

(3) The ship is sufficiently "slender" so that each section can be treated as a two-dimensional "strip" with no interaction between them;

(4) The response of the ship to the incident wave is linear.

Let Oxyz be a right-handed rectangular coordinate system translating with the mean position of the ship. The origin is located on the calm water surface. The x-axis points forward and the z-axis points vertically upward.

Let Φ be the velocity potential given by:

$$\Phi(x,y,z,t) = -Ux + \phi(x,y,z,t) \qquad (2.1)$$

---

*References are listed on page 23

and the absolute velocity of the fluid is described by:

$$\underset{\sim}{q}(x,y,z,t) = \nabla\Phi = -U\underset{\sim}{e}_1 + \nabla\phi, \tag{2.2}$$

where $\nabla\phi = \underset{\sim}{v} = u\underset{\sim}{e}_1 + v\underset{\sim}{e}_2 + w\underset{\sim}{e}_3$ represents the perturbation fluid velocity, and $\underset{\sim}{e}_1$, $\underset{\sim}{e}_2$ and $\underset{\sim}{e}_3$ the three unit vectors in Oxyz frame. For convenience, the perturbation potential ϕ is decomposed into a steady part ϕ_S and a time-dependent part ϕ_T, i.e.,

$$\phi(x,y,z,t) = \phi_S(x,y,z) + \phi_T(x,y,z,t) \tag{2.3}$$

where ϕ_S describes the disturbance due to the steady forward motion of the ship in calm water and ϕ_T can be further decomposed as:

$$\phi_T = \phi_I + \phi_D + \phi_M = \phi_I + \phi_B \tag{2.4}$$

where ϕ_I is the potential of the incoming plane progressive wave, ϕ_D the diffraction potential due to the presence of the ship, and ϕ_M the forced-oscillation potential. The incoming wave potential ϕ_I is given by:

$$\phi_I = \mathrm{Re}\{\, \psi_I(x,y,z)\exp(i\omega t)\,\}, \tag{2.5}$$

where

$$\psi_I = -\frac{Ag}{\sigma}\exp\{k_0 z - ik_0(x\cos\beta + y\sin\beta)\} \tag{2.6}$$

in which A is the wave amplitude, σ the wave frequency, $k_0 = \sigma^2/g$ the wave number, β the wave heading angle counted from the positive x-axis in the counterclockwise direction, g the gravitational acceleration and ω the frequency of encounter. Note that a ship advancing through regular sinusoidal wave will not respond at the frequency of incoming wave, instead at the frequency of encounter which is defined as:

$$\omega = \sigma - k_0 U\cos\beta\ . \tag{2.7}$$

Under the assumption of linear response, we have

$$\phi_B = \mathrm{Re}\{\ \psi_B(x,y,z)\exp(i\omega t)\ \}. \tag{2.8}$$

From the linear momentum consideration we can derive the force, and by taking the time average of the force, the second-order steady forces $<\Delta F>$ are obtained in terms of $\psi_B\psi_I^*$ and $\psi_B\psi_B^*$ where "*" indicates the complex conjugate. By repeated application of the method of stationary phase at a large distance from the ship and after lengthy algebraic manipulation, the following results are obtained:

$$<\Delta F> = <\Delta F_{IB}> + <\Delta F_{BB}> \tag{2.9}$$

where

$$<\Delta F_{IB}> = \frac{1}{2}\rho g A \begin{pmatrix}\cos\beta\\ \sin\beta\end{pmatrix} \mathrm{Im}\{\ H(\beta,k_0)\ \}, \tag{2.10}$$

$$<\Delta F_{BB}> = -\frac{\rho}{8\pi}\left(\int_{-\pi/2}^{\pi/2} - \int_{\pi/2}^{\pi-u_o} - \int_{\pi+u_o}^{2\pi}\right) du\ \frac{\lambda_1^2(u)}{(1+4\tau\cos u)^{1/2}} \begin{pmatrix}\cos u\\ \sin u\end{pmatrix} |H(\pi+u,\lambda_1)|^2$$

$$-\frac{\rho}{8\pi}\left(\int_{0}^{\pi-\mu_o} + \int_{\pi+u_o}^{2\pi}\right) du\ \frac{\lambda_2^2(u)}{(1+4\tau\cos u)^{1/2}} \begin{pmatrix}\cos u\\ \sin u\end{pmatrix} |H(\pi+u,\lambda_2)|^2 \tag{2.11}$$

in which

$$u_0 = \begin{cases} 0 & , \tau \le 1/4 \\ \cos^{-1}(1/4\tau), & \tau > 1/4 \end{cases},$$

cos u and cos β correspond to the added resistance and sin u and sin β correspond to the lateral drift force. The Kochin function, $H(u,\lambda)$, and λ_1, λ_2 will be explained in the next section in detail.

As shown in Equations (2.10) and (2.11) the forces are the second-order quantities, because according to the usual formulation of the ship motion

problem the velocity potentials are considered as the first order of the wave amplitude and so is the Kochin function (see Equation (3.1)).

KOCHIN FUNCTION

The function $H(u,\lambda)$ known as the Kochin function is defined as follows:

$$H(u,\lambda) = \iint_{S_{BO}} \left(\frac{\partial \psi_B(\underset{\sim}{x}_0)}{\partial n} - \psi_B(\underset{\sim}{x}_0) \frac{\partial}{\partial n} \right) \exp\{\lambda_p z_0 + i\lambda_p (x_0 \cos u + y_0 \sin u)\} ds \tag{3.1}$$

Here the integration is over the mean position of the hull surface S_{BO}, and

$$\lambda_p = \frac{\nu}{2\tau^2 \cos^2 u} \{1 + 2\tau \cos u \pm (1+4\tau \cos u)^{1/2}\}, \quad p=1,2 \tag{3.2}$$

where $\nu = \omega^2/g$, $\tau = U\omega/g$, and the plus and minus signs are for p=1 and p=2, respectively. Figure 2 shows the behavior of λ_1 and λ_2 as a function of u.

Let us first consider the ship-generated potential ψ_B in detail. Using the principle of linear superposition we can expand ψ_B, and hence the Kochin function as follows:

$$\psi_B = \sum_{i=1}^{6} \alpha_i \psi_i + \psi_D, \tag{3.3}$$

where α_i is the displacement of the body due to the motion in the ith mode, and i=1,2,3,4,5,6 represent surge, sway, heave, roll, pitch and yaw, respectively and

$$H(u,\lambda) = \sum_{i=1}^{6} \alpha_i H_i + H_D. \tag{3.4}$$

The potential ψ_i when multiplied by the complex amplitude α_i represents the fluid disturbance due to the body oscillation in the ith mode, and so does the Kochin function. We can easily note from Equations (2.10),(2.11) and (3.1) that it is very important to predict the ship motion and diffraction potential accurately, because the second-order forces are expressed

in terms of the Kochin function, and the Kochin function itself could be obtained by the integration of ψ_i and ψ_D over the mean body surface S_{BO}. Therefore, small errors in the prediction of ship motion and the potentials ψ_i and ψ_D could result in large errors in the forces.

SHIP MOTION PROBLEM

Our ship motion computation has been developed on the basis of the method of Salvesen et al.(1970). A brief review of the typical assumptions which are required for the theoretical justification of the strip theory, will be given first.

The hull is assumed to be long and slender such that if B is a typical transverse dimension and L is the length, then

$$B/L = O(\varepsilon), \tag{3.5}$$

and

$$n_1 = O(\varepsilon),\ n_2 = O(1) \text{ and } n_3 = O(1) \tag{3.6}$$

where n_1, n_2, and n_3 are components of unit normal vector on the immersed ship surface. It follows that in the neighborhood of the hull

$$\frac{\partial}{\partial x} = O(\varepsilon),\ \frac{\partial}{\partial y} = O(1) \text{ and } \frac{\partial}{\partial z} = O(1). \tag{3.7}$$

In addition we shall make a crucial assumption that the frequency of encounter is high, $\omega >> U\frac{\partial}{\partial x}$, which means that the wave length is approximately of the same order of B. All these assumptions could only be justified by comparing solutions with experimental data. We will summarize the above assumptions in the following manner.

Original	With Assumption	
Field equation		
$\left(\frac{\partial^2}{\partial x^2}+\frac{\partial^2}{\partial y^2}+\frac{\partial^2}{\partial z^2}\right)\psi_i=0$	$\left(\frac{\partial^2}{\partial y^2}+\frac{\partial^2}{\partial z^2}\right)\psi_i=0$	(3.8)
Free surface condition		
$(\omega^2-i\omega U\frac{\partial}{\partial x}-U^2\frac{\partial^2}{\partial x^2})\psi_i-g\frac{\partial}{\partial z}\psi_i=0$	$\omega^2\psi_i-g\frac{\partial}{\partial z}\psi_i=0$	(3.9)
Body boundary condition		
$\frac{\partial\psi_i}{\partial n}=i\omega n_i+Um_i$	$\frac{\partial\psi_i}{\partial N}=i\omega N_i+Um_i$	(3.10)
Radiation condition		
$\lim_{R\to\infty} R^{1/2}\left(\frac{\partial\psi_i}{\partial R}-ik_0\psi_i\right)=0$	$\lim_{y\to\pm\infty}\left(\frac{\partial\psi_i}{\partial y}\pm ik_0\psi_i\right)=0$	(3.11)

where $R=(x^2+y^2)^{1/2}$ and n_i is defined by

$$(n_1,n_2,n_3)=\underset{\sim}{n} \quad \text{and} \quad (n_4,n_5,n_6)=\underset{\sim}{r}\times\underset{\sim}{n}$$

with $\underset{\sim}{n}$ the unit normal vector which is directed into the body and $\underset{\sim}{r}$ the position vector with respect to the origin of the coordinate system and where $m_i=0$ for $i=1,2,3,4$ while $m_5=n_3$ and $m_6=-n_2$. N_i is the 2-dimensional generalized normal in the y-z plane. We note that with the above assumptions, ψ_i does not depend on the x-coordinate explicitly. Introducing the assumptions into Equation (3.1) and setting ds=dxdl, we can also show that

$$H_i(u,\lambda) = \int_L dx\ \exp(i\lambda x\cos u) \int_{C(x)} dl\ \{\ \frac{\partial \psi_i}{\partial N} - (\ \psi_i + \frac{U}{i\omega}\ \psi_i^U\ )\frac{\partial}{\partial N}\ \}$$

$$\times\ \exp\{\ \lambda(z + iy\sin u)\ \},\qquad (3.12)$$

in which C(x) is the immersed contour of the cross section of the ship at station x, and using body boundary condition(3.10), we may obtain

$$H_i(u,\lambda) = \int_L dx\ \exp(i\lambda x\cos u) \int_{C(x)} dl\{(i\omega n_i + U m_i) - (\psi_i + \frac{U}{i\omega}\ \psi_i^U)$$

$$\times\ \lambda\ (N_3 + iN_2\sin u)\}\exp\{\lambda(z+iy\sin u)\}.\qquad (3.13)$$

where $\psi_i^U = 0$ for i=1,2,3,4, $\psi_5^U = \psi_3$ and $\psi_6^U = -\psi_2$.

Naturally in order to calculate the Kochin function the velocity potential ψ_i which satisfies Equations (3.8) to (3.11) must be obtained beforehand. There are several methods in use for finding solutions for this boundary-value problem such as separation of variables and the Fourier method, the method of reduction and reflection, the method of Green's functions, the method of multipole expansion, and so on. Among them the method of Green's functions is certainly the most flexible one. The solution by this method involves an integral equation, i.e.,

$$\psi(P) = \frac{1}{2\pi}\int_{C(x)} \{\psi_\nu(Q)G(P,Q) - \psi(Q)G_\nu(P,Q)\}\ ds(Q),\qquad (3.14)$$

where P = (y,z), Q = (y_0,z_0), ν the normal derivative in terms of (y_0,z_0), C(x) a contour bounding a two-dimensional region, ds the arc length and Green's function which we denote G(P,Q) satisfies the following equations:

$$(\ \frac{\partial^2}{\partial y^2} + \frac{\partial^2}{\partial z^2}\ )\ G(P,Q) = \delta(y-y_0)\ \delta(z-z_0)\ ,\qquad (3.15)$$

$$\omega^2 G(y,0;y_0,z_0) - g \frac{\partial}{\partial z} G = 0 , \tag{3,16}$$

$$\lim_{y\to\pm\infty} \{ \frac{\partial G(y,0;y_0,z_0)}{\partial y} \pm ik_0 G \} = 0. \tag{3.17}$$

and the solution is as follow (see Wehausen and Laitone,1960) :

$$G(P,Q) = \log(r) + \log(r') - 2PV\int_0^\infty \frac{\exp k_0(z+z_0) \cos k_0(y-y_0)}{k-k_0} dk + 2\pi i \times \exp[k_0(z+z_0)\cos(k_0(y-y_0))] \tag{3.18}$$

in which $r = \{(y-y_0)^2 + (z-z_0)^2\}^{\frac{1}{2}}$, $r' = \{(y-y_0)^2 + (z+z_0)^2\}^{\frac{1}{2}}$, $k_0=\omega^2/g$ and PV indicates the Cauchy principal-value integral.

Although one can show in many cases that a solution to the integral equation exists, a closed form solution is usually not obtainable, and the only possible way to solve it is by numerical solution. With the advent of high-speed computers, a numerical solution of integral equations has become almost a routine procedure. However, one major drawback in solving an integral equation of the second kind is the non-uniqueness of the solution when the homogeneous part of the equation has nontrivial eigen values. For a body floating in a free surface, John (1950) pointed out that the integral equation involved admits non-unique solutions at the eigen-frequencies. He called these eigen-frequencies irregular frequencies. The problem of irregular frequencies has received extensive investigations. Paul Wood has demonstrated by numerical computation (ref. Paulling, 1970) that the irregular frequencies can be removed by extending the source distribution onto the waterline inside the cylinder and imposing a rigid wall condition on it (see Figure 3). Frank (1967)

studied these irregular frequencies numerically for two-dimensional cylinders and found that the matrix becomes ill-conditioned at and within a narrow band near irregular frequencies. The problem is important because these irregular frequencies are not known a priori for a complicated geometry. Ohmatsu (1975) has shown how to avoid this difficulty by modifying the interior problem and proved Paul Wood's justification by using Green's theorem. Ogilvie and Shin (1978) have presented a rather simple procedure that could eliminate irregular frequencies by making a minor change in the Green's functions based on a procedure suggested by Ursell (1953).

The reason we gave some detailed explanation for computation procedure is that the prediction of the second-order steady forces requires the ship motion response and the diffraction potential as input values, so that the second-order steady forces predicted by a given method may vary considerably depending on the method used for obtaining the motion and the diffraction potential as also mentioned in Salvesen (1976). In our computation we adopt Frank's close-fit method but we avoid irregular frequencies by adding a horizontal rigid wall inside the body by following Paul Wood's method. Figure 4 shows the heave added-mass coefficients of a circular cylinder with and without a horizontal wall. Figure 5 displays the added-mass, damping coefficients and heave, pitch magnitudes for a Mariner hull form.

DIFFRACTION PROBLEM

For the diffraction part of Kochin function $H_D(u,\lambda)$, we cannot immediately follow the expression of Kochin function $H_I(u,\lambda)$ for the forced motion in Equation (3.13). Before writing down the desired final form, let us study the diffraction problem in some detail.

With the incident-wave potential given by Equation (2.6), the diffraction potential ψ_D is subject to the condition that the total potential $\psi_I+\psi_D$ has zero normal velocity on the body surface. Since the incident wave has the factor $\exp(-ik_0 x\cos\beta)$, it seems reasonable to expect that for a slender ship and short waves the diffraction waves

also have similarly oscillatory behavior along the x-axis. This assumption is not valid near the ends, but then the assumptions we made, i.e., n_x changes slowly in the x-direction is not valid there either. It is for this reason that we may write

$$\psi_D = \Psi_D(y,z)\exp(-ik_0 x\cos\beta). \tag{3.20}$$

With this definition Ψ_D must satisfy the following equations:

$$\Psi_{Dyy} + \Psi_{Dzz} + (-ik_0\cos\beta)^2\Psi_D = 0, \tag{3.21}$$

$$\omega^2\Psi_D(y,0) - g\Psi_{Dz} = 0, \tag{3.22}$$

$$\frac{\partial\Psi_D}{\partial n} = -\frac{\partial\psi}{\partial n} = A\omega(N_3 - iN_2\sin\beta)\exp\{k_0(z-iy\sin\beta)\}, \tag{3.23}$$

$$\lim_{y\to\pm\infty}\left(\frac{\partial\Psi_D}{\partial y} \pm ik_0\Psi_D\right) = 0. \tag{3.24}$$

Equation (3.21) is known as Helmholtz equation. Newman(1970) showed that the determination of the sectional forces due to the incident waves should deal with a Helmholtz equation in the cross plane instead of Laplace's equation as the usual strip theory does. But it is not an easy task to solve a Helmholtz equation with boundary conditions (3.22) to (3.24). Choo (1975) solved the Helmholtz equation and obtained the diffraction potential by using an asymptotic series expansion technique for the case of zero speed and Troesch (1976) tried to extend to that forward motion at moderate speeds without obtaining numerical values. Troesch compared his numerical computation with not only experimental data but also the solution of the same boundary value problem, using two-dimensional Laplace's equation as the governing equation. Figure 6 shows the pressure distribution for the midship section of an

ore carrier for $L/\lambda = 1.96$ and $\beta=135^{o}$, 45^{o}. The integrated pressure forces are presented in Table 1. F_y and F_z are the amplitude of the sectional exciting forces in the horizontal and vertical directions respectively and are nondimensionalized with respect to $\rho gAB/2$ where B is the sectional beam.

	Helmholtz		Laplace	
	magnitude	phase (Deg)	magnitude	phase (Deg)
$\frac{F_y}{\rho gAB/2}$	1.11	120	0.95	115
$\frac{F_z}{\rho gAB/2}$	0.49	-55	0.47	-57

TABLE 1 Sectional Exciting Force

In Figure 7 total forces which are integrated over the hull for the Series 60, $C_B = 0.70$ are plotted for heading angle $\beta=150^{o}$ and $\omega(B/2g)^{\frac{1}{2}}$ ranging from 0.6 to 1.2.

In spite of the more elaborate numerical computation involved in the solution of the Helmholtz equation compared to the solution of Laplace's equation, the results do not seem to be so different from those of Laplace's equation as to influence practical predictions. Thus, we shall adopt Laplace's equation in our computation, but we have to keep in mind that neglecting the$(-ik_0\cos\beta)^2$ term in Equation (3.21) violates the crucial assumption we made for the justification of the strip theory in ship motion, i.e., $\lambda/L = 0(\epsilon)$. Replacement of the Helmholtz equation by the Laplace's equation saves considerable amount of computing time, because once we solve the forced motion problem numerically, we can immediately

* In Troesch $\beta=0$(degree) for head seas.

obtain the diffraction potentials by simply changing body boundary condition. Numerical procedure for this simplification will be given in the following section. In passing, the Kochin function for the diffraction part will be expressed as:

$$H_D(u,\lambda) = \iint_{S_{Bo}} ds\left(\frac{\partial \psi_D}{\partial n} - \psi_D \frac{\partial}{\partial n}\right) \exp\{\lambda(z+ix\cos u+iy\sin u)\}$$

$$\simeq A\omega \int_L dx\, \exp\{ix(\lambda\cos u - k_0\cos\beta)\} \int_{C(x)} dl\,(N_3 - iN_2\sin\beta)$$

$$x\, \exp\{(k_0+\lambda)z + iy(\lambda\sin u - k_0\sin\beta)\}$$

$$-\int_L dx\, \exp(i\lambda x\cos u) \int_{C(x)} dl\; \lambda\psi_D(N_3 + iN_2\sin u)$$

$$x\, \exp(\lambda z + i\lambda y\sin u)\,.$$

NUMERICAL PROCEDURE

As mentioned earlier, Frank (1967) solved the two-dimensional problem where the logarithmic sources of Equation (3.18) were distributed over the hull cross section. Using the method of linear superposition, one can express the potential Ψ by

$$\psi(P) = \int_C \sigma(Q) G(P,Q)\, dl(Q) \qquad (3.26)$$

with the unknown source strength $\sigma(Q)$.

In order to solve Equation (3.26) two assumptions are introduced in the numerical method. As shown in Figure 8 a hull cross section is described by n offsets where dl_j is the arclength between the j and j+1 points.

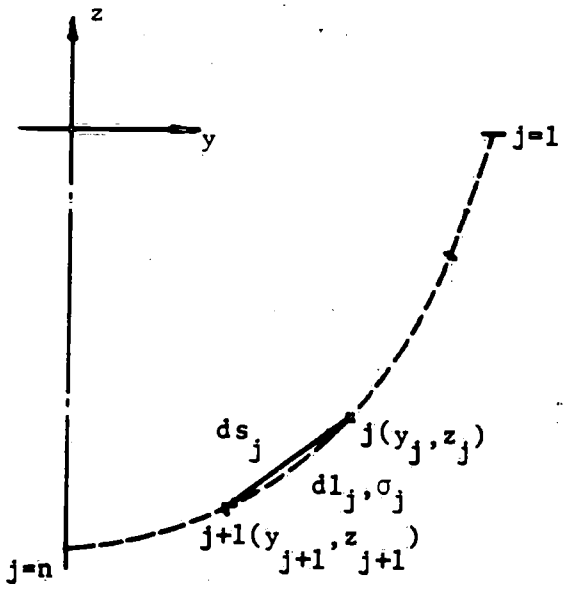

Figure 8 - Cross Section of Hull

The first assumption is that the source strength $\sigma(l)$ varies slowly enough to be considered as constant σ_j over a given arclength dl_j. The second assumption is that arc dl_j can be substituted by a straight line ds_j such that the ship section could be approximated by a chain of straight lines.

With these assumptions and body boundary condition (3.10), one can obtain the following expression:

$$\frac{\partial}{\partial N}\psi(\bar{P}_i) = \sum_{j=1}^{n-1} \frac{\partial}{\partial N}\int_{dl_j} \sigma(Q)G(\bar{P}_i,Q)dl(Q)$$

$$\approx \sum_{j=1}^{n-1} \sigma_j \frac{\partial}{\partial N}\int_{dl_j} G(\bar{P}_i,Q)dl(Q)$$

$$\approx \sum_{j=1}^{n-1} \sigma_j \frac{\partial}{\partial N}\int_{ds_j} G(\bar{P}_i,Q)ds(Q) \qquad (3.27)$$

where σ_j is the constant source strength between points j and j+1, $\bar{P}_i$ the midpoint of the i-th arc. Using matrix notation, we may have

$$f_i = \sum_{j=1}^{n-1} A_{ij}\sigma_j , \qquad i=1,2,\cdots,n-1 \tag{3.28}$$

where $f_i = \frac{\partial}{\partial N}\psi(\bar{P}_i)$ and $A_{ij} = \frac{\partial}{\partial N}\int ds_i G(\bar{P}_i,Q)ds(Q)$. The advantage of Equation (3.27) is that the term $\frac{\partial}{\partial N}\int G\, dl$ can be evaluated in a closed form. By increasing the number of offset points this approximation approaches the exact solution. However numerical computations show that a relatively small number of points, for example 15 points for a half circle, gives fairly good agreement with the exact solution. We also may increase the accuracy of solution either by assuming linearly varying source strength over the line segments ds_i for a fixed number of offset points, or by integrating along an arc dl_i instead of ds_i with constant or linear σ_i. But the increased numerical complexity may offset its merit.

From Equations (3.27) and (3.28) we can note that for given frequency ω and contour C(x) the coefficient matrix A_{ij} of the forced motion or diffraction problem is the same. Therefore once we obtain the inverse of matrix A_{ij}, forced motion and diffraction can be solved simultaneously. This is the consequence of replacing the Helmoltz equation by the two-dimensional Laplace's equation.

THE SECOND-ORDER STEADY FORCES

Before calculating the forces, let us discuss the numerical procedure for the Kochin function first. The general form of the Kochin function H may be written as:

$$H(\lambda's) = \int_L dx\, \exp(i\lambda_1 x)\int_{C(x)} dl\, f(x;y,z)\exp(\lambda_2 z + i\lambda_3 y), \tag{3.29}$$

where L is the ship length and f(x;y,z) has x as a parameter. If we assume that f (x;y,z) varies smoothly over C(x), then for the contour integral we might adopt the same assumptions as Frank did. That is,

$$\int_{C(x)} dl\ f(x;y,z)\exp(\lambda_2 z+i\lambda_3 y)$$

$$\approx \sum_{j=1}^{n-1} f(x;\bar{y}_j,\bar{z}_j)\int_{ds_j} ds\ \exp(\lambda_2 z+i\lambda_3 y). \qquad (3.30)$$

Given N_s stations along ship length, we may calculate the integral (3.30) at $x=X_j$ and denote its value as $F(X_j;\lambda_2,\lambda_3)$ and from Equation (3.29) we get,

$$H(\lambda's) = \int_L dx\ \exp(i\lambda_1 x)S_i(x), \quad \text{for } i=1,2,\cdots,N_s. \qquad (3.31)$$

where $S_i(X)$ is the function to be obtained by curve fitting $F(X_i;\lambda_1,\lambda_2)$ Now it is plausible to find a method for obtaining a smooth representation for the discrete data $F(X_i;\lambda_1,\lambda_2)$ by the use of the spline function method of curve fitting. By using this method we may define the interpolating spline as

$$S_i(x) = a_i(x-X_i)^3 + b_i(x-X_i)^2 + c_i(x-X_i) + d_i, \qquad (3.32)$$

in the interval $X_i \le x \le X_{i+1}$. The coefficients of the cubic polynomial are expressed in terms of $F(X_i;\lambda_1,\lambda_2)$, $F(X_{i+1};\lambda_1,\lambda_2)$, and the second derivatives $S_i''(X_i), S_i''(X_{i+1})$ (see Appendix A). Consequently we may rewrite the Equation(3.31) as follows:

$$H(\lambda's) = \sum_{i=1}^{N_s-1}\int_{X_i}^{X_{i+1}} dx\ \exp(i\lambda_1 x)S_i(x). \qquad (3.33)$$

This integration can be performed exactly.

Equation(2.9) shows that the second-order steady force consists of two terms, $\langle\Delta F_{IB}\rangle$ and $\langle\Delta F_{BB}\rangle$. The computation of $\langle\Delta F_{IB}\rangle$ is straightforward for a given $u=\beta$ and $\lambda=k_0$. On the other hand, $\langle\Delta F_{BB}\rangle$ in Equation (2.11) is rather complicated. The reason is that the Kochin function is a function of u,λ_1,λ_2; furthermore, λ_1,λ_2 themselves are function of u. Figure 2 shows that the λ_1 goes to infinity as u approaches to $\pi/2$.

The evaluation of the Kochin function becomes more difficult as λ_1 becomes large, for the integrand of the Kochin function oscillates very rapidly along the x and y axes for large values of λ_1. In the computation we first decide the angle u_ε which satisfies the following (see Appendix B):

$$\left(\int_{-\pi/2}^{\pi/2} - \int_{\pi/2}^{\pi-u_o} - \int_{\pi+u_o}^{3\pi/2}\right) du\ D(u,\lambda_1)$$

$$\simeq \left(\int_{-\pi/2+u_\varepsilon}^{\pi/2-u_\varepsilon} - \int_{\pi/2+u_\varepsilon}^{\pi-u_o} - \int_{\pi+u_o}^{3\pi/2-u_\varepsilon}\right) du\ D(u,\lambda_1)$$

where $D(u,\lambda_1) = \dfrac{\lambda_1^2(u)}{(1+4\tau\cos u)^{1/2}} |H(\pi+u,\lambda_1)|^2 \begin{pmatrix}\cos u\\ \sin u\end{pmatrix}$.

By doing this we may partly eliminate the difficulty involved in the force integral. The contribution of each mode of ship motion and the diffraction part to the force is examined separately. The numerical results comparing their relative magnitude (see Figure 13) shows that the major source of the forces are from heave and pitch.

The computer program based on Lin and Reed's theory has been developed by Reed and Hubble(1980) originally. Extensive debugging and modification that includes the irregular frequency in ship motion problem, the diffraction problem and the force integral are made by author. All the methods has been synthesized into single computer program by essentially combining the ship motion program and the Kochin function evaluation. The ship motion program consists of several links, and the Kochin function is the last link to the ship motion program.

NUMERICAL RESULTS

It is obvious that computational accuracy increases with the number of elements used to approximate the body surface, and, in the meanwhile, that the cost for a solution depends very strongly on the number of points used. The source points should be distributed in such a way that the best results will be obtained with the fewest possible points. Naturally, points should be concentrated in regions where the flow is expected to change rapidly. In order to decrease the computing cost within the tolerable

limit of accuracy we took the following steps: first, we tried to obtain the optimal minimal number of offset points on the body. Second, within the range of frequency of practical interest appropriate intervals of frequencies are taken at which the potential, added-mass coefficient, damping coefficient, and etc. are evaluated, and the linear interpolation method is used to get those values at the frequencies between the initially chosen frequencies. Lastly, the integral of equation (2.10) was also approximated by a finite sum of discretized integrals.

The computations were mostly carried out on the CDC 6600, 6700 computer at DTNSRDC. The evaluation of the influence coefficient matrix for the singularity strength and the evaluation of the Kochin function were the most time consuming parts of these computations.

Numerical Examples

To facilitate the comparison, the added resistance and the lateral drift force were non-dimensionalized as follows:

$$\Delta F_x = \frac{\text{added resistance}}{\rho g A^2 B^2 / L} \qquad (4.1)$$

A = incident wave amplitude
B = Beam
L = Shiplength

$$\Delta F_y = \frac{\text{lateral drift force}}{\rho g A^2 L} \qquad (4.2)$$

Figure 9 shows the added-resistance prediction for a Mariner hull form at a speed of $F_n = 0.194$ with three different headings, $\beta = 120^\circ$, 150° and 180° (Note that $\beta = 180^\circ$ for head seas). A striking fact to note is that the extreme sensitivity of the added resistance to the heading angles. For instance, at $\lambda/L = 0.6$ which corresponds to approximately 300 feet wave length, the added resistance can increase about 6 times when the wave heading angle is changed from the 30° bow to 60° bow. The results in Figure 9 reveal that the usual notion that the added resistance is greater in head seas is not necessarily true. In Figure 10 comparisons were made between Salvesen's calculation and $\langle F_{IIB} \rangle$ at $F_n = 0.194$. The major

differences between Salvesen (1978) and the present theory is that Slavesen ignored $\langle \Delta F_{1BB} \rangle$ in Equation(2.9) by assuming $\psi_B \ll \psi_I$. Relatively good agreement in magnitude is observed, but there still exists discrepancy between them. There might be two reasons for this; first, in developing the ship motion program some modifications were made on the Frank's close-fit method as mentioned earlier. Secondly, the computation of the diffraction part is quite different. In Figure 11 we note that $\langle \Delta F_{1BB} \rangle$ compared with $\langle \Delta F_{1IB} \rangle$ is not small enough to be neglected. Figure 12 displays the contribution of the forced motion and the diffraction part to the force $\langle \Delta F_{1IB} \rangle$ separately for the three different headings at $F_n = 0.194$. As would be expected, it is seen that the effects of the forced motion decrease as λ/L becomes large, and the maximum occurs at shorter wavelength for decreasing heading angles. Meanwhile, the diffraction part seems to act differently to that of the forced motion.

Figure 13 shows relative magnitudes of each mode of ship motion for $\langle \Delta F_{1IB} \rangle$ separately. Pitch and heave are dominant over the others. It is interesting to note that the peak values of pitch and heave for $\beta = 150^\circ$ are slightly greater than those for $\beta = 180^\circ$. These effects are reflected in Figure 12 where the peak value of the added resistance for $\beta = 150^\circ$ is slightly greater than those for $\beta = 180^\circ$. $\langle \Delta F_{1BB} \rangle$ is presented in Figures 14 and 15. Basically $\langle \Delta F_{1BB} \rangle$ consists of two integrals, i.e., λ_1, $_2$ and the corresponding Kochin functions $H(u,\lambda_1)$, $H(u,\lambda_2)$ respectively. As expected, Figure 14 shows that we might neglect the highly oscillatory λ_1 integral in the computation. In Figure 15, $\langle \Delta F_{1BB} \rangle$ is expressed in terms of each ship-motion mode, diffraction and their interactions.

The usefulness of any theory cannot be judged until its prediction have been compared with empirical data. Unfortunately, it is difficult to find experimental data, especially in an oblique seaway. We selected one of the available experimental data; Series 60, $C_B = 0.60$ at $F_n = 0.283$ in head seas. In Figure 16 the theoretical predictions of three different methods are presented together with two sets of experimental data obtained by Sibul (1971) and Strom-Tejsen et al. (1973) for this particular case.

oblique = inclined not parallel nor perpendicular.

All numerical values overpredict Added Resistance

In the lower frequency ranges not only do all three numerical predictions agree well with each other, but also they show fairly good agreement with the experimental values. All the numerical values overpredict the maximum added resistances, however. Gerritsma and Beukelman(1972) overpredict it by about a factor of two, the present theory by nearly 70% and Salvesen's method by approximately 35%. In the higher frequency ranges the present theory gives a little better prediction when compared to the others. It is probably because our computation of the diffraction potential, which is the major contribution to the added resistance in the higher frequency ranges, is better than others. Two interesting things are observed for $\langle \Delta F_{1IB} \rangle$; first, $\langle \Delta F_{1IB} \rangle$ for this case show good agreement with experimental data. Secondly $\langle \Delta F_{1IB} \rangle$ is slightly higher than the added-resistance of Salvesen for a Mariner but much less than that of Salvesen for Series 60. We cannot give any specific reasons for the descrepancies. Only by comparing both methods term by term, we may find out the differences.

The lateral drift forces for a Mariner are also presented in Figures 17 and 18. Figure 17 shows the lateral drift force, $\langle \Delta F_2 \rangle$, with three different headings $\beta = 90^0$, 120^0, 150^0. As would be expected, the coefficient approaches 0.5 as the frequency becomes higher for the beam-sea case, but the predictions give small negative values for oblique seas in the higher frequency ranges. $\langle \Delta F_{2IB} \rangle$ and $\langle \Delta F_{2BB} \rangle$ are plotted separately in Figure 18. The relative magnitude of $\langle \Delta F_{2BB} \rangle$ compared with $\langle \Delta F_{2IB} \rangle$ is much smaller than that of $\langle \Delta F_{1BB} \rangle$ with $\langle \Delta F_{1IB} \rangle$. Comparisons of added resistance and lateral drift force with experimental values will be given in the future.

CONCLUDING REMARKS

The second-order steady forces have been considered for a ship in regular waves of arbitrary headings. The accurate prediction of these forces is of considerable importance for estimating the powering requirement in waves, assessment of seakeeping qualities, and the position control of ships. Based on Lin and Reed (1976) a new numerical scheme has been developed for predicting the added resistance and drift force.

The summary of the findings in this study is as follows:

(1) It is not so easy to verify the computed second-order steady forces satisfactorily because of the lack of reliable experimental data.

(2) The effect of wave heading on added resistance is significant. The maximum added resistance does not necessarily occur in the head seas only.

(3) For decreasing heading angle or λ/L, the contribution of the motion to the added resistance decreases while that of the diffraction part increases;

(4) There exists a contradiction between the assumptions made in ship motion and the diffraction problem. In the ship motion problem the justification of the strip theory is made by assuming $\lambda=O(B)$, i.e., the wavelength is approximately of the order of B, while in diffraction problems the term $(k^2\cos^2\beta)$ is dropped in order to replace the Helmholtz equation by Laplace's equation. That means that in the diffraction problem the assumption of $\lambda \gg B$ is made.

It is fair to say that the theory of Lin and Reed is mathematically sound, but there still exists a gap between the theory and its practical applicability. In concluding this work we like to make some suggestions for future study. First of all, to develop a numerical prediction method of the second-order steady forces it is desired to use the most accurate method for predicting ship motion. For the diffraction problem we have to solve either three-dimensional Laplace's equation or Helmholtz equation in high frequency ranges.

ACKNOWLEDGEMENT

Since this work had been initiated by Arthur M. Reed and E. Nadine Hubble several years ago, they already developed most of the computer program when I took over this problem in 1979. I would like to expressed my sincere gratitude to them for their enormous effort on the computer program.

I would like to thank Dr. Choung M. Lee who gave invaluable suggestions and insights into the problem on various occasions. I am also indebted to Dr. Joe W.-C. Lin for his enthusiastic discussions and friendly help.

REFERENCES

Choo,K.Y., Exciting Forces and Pressure Distribution on a Ship in Oblique Wave. Ph.D. Dissertation, Massachusetts Institute of Technology,1975.

Frank,W., Oscillation of Cylinder In or Below the Free Surface of Deep Fluid. NSRDC Rep. 2375, 40pp. 1967.

Gerritsma,J. and Beukelman,W., Analysis of the Resistance Increase in Waves of a Fast Cargo Ship. International Shibuilding Progress, Vol.19 pp.285-293, 1972.

John,F., On the Motion of Floating Bodies, I and II. Commun. Pure Appl. Math. 2:13-57, 3:45-101, 1950.

Lin,W.C. and Reed,A.M., The Second-Order Steady Force and Moments on a Ship Moving in an Oblique Seaway. The Office of Naval Research, 11th Symp. on Naval Hydrodynamics, London, 1976.

Newman,J.N., Application of Slender-Body Theory in Ship Hydrodynamics, Annual Review of Fluid Mechanics, 2:67-94, 1970.

Ohmatsu,S., On the Irregular Frequencies in the Theory of Oscillating Bodies in a Free Surface. Papers of Ship Research Inst.,No.48, 1975.

Ogilvie,T.F. and Shin,Y.S., Integral Equation Solution for Time-Dependent Free-Surface Problem. J. Soc. Naval Arch. Japan, Vol. 143, 1978.

Paulling,J.R., Stability and Ship Motion in a Seaway, Summary Rep. 1 July, 1969-30 June, 1970, Coast Guard.

Reed,A.M. and Hubble,E.N., Program Force, Added Resistance and Drifting Forces in Waves, User's Manuel. DTNSRCD/SPD-0890-01, June, 1980.

Salvesen,N., Tuck,E.O. and Faltinsen,O., Ship Motion and Sea Loads. Trans. Soc. Naval Arch. Marine Engs., Vol. 78, pp250-279; discussion pp279-287, 1970.

Salvesen,N., Added Resistance of Ships in Waves. J. Hydronautics, Vol. 12, No. 1, Jan. 1978, pp24-34.

Sibul,O.J., Measurements and Calculation of Ship Resistance in Waves. College of Engineering, Univ. of Calif., Berkeley, Rep.No.NA-71-2,1971.

Strom-Tejsen,T., Yeh,H.Y.H., and Moran,D.D., Added Resistance in Waves, SNAME, Transactions, Vol. 81, 1973, pp109-143.

Troesch,A.W., The Diffraction Potential for a Slender Ship Moving through Oblique Waves. PhD Thesis, University of Michigan, Ann Arbor, 1976.

Wehausen,J.V. and Laitone,E.V., Surface Waves. Encyclopedia of Physics, Vol. 9, pp446-778, Springer-Verlage, Berlin, 1960.

APPENDIX A

Spline Curve Fitting

Suppose we wish to approximate a continuous and differentiable function $F(x)$ on the interval $\{0,L\}$ in a piecewise fashion, using low-degree interpolating polynomials over nonoverlapping subintervals of $\{0,L\}$. Let the base points be $0 = x_o < x_1 < \ldots x_{n-1} < x_n = L$, the corresponding functional vaules be $y_i=F(x_i)$, $i=0,1,2,\ldots,n$, and interpolating function for $\{0,L\}$ be $S_i(x)$. We shall require that $S_i(x)$ be continuous on $\{0,L\}$ and possess continuous first and second derivatives for all x in $\{0,L\}$. Let $S_i(x)$ coincide with a third-degree polynomial on each interval, i.e.,

$$S_i(x) = a_i(x-X_i)^3 + b_i(x-X_i)^2 + c_i(x-X_i) + d_i, \quad (A.1)$$
$$(\ X_i \leq x \leq X_{i+1}\ )$$

then

$$S_i'(x) = 3a_i(x-X_i)^2 + 2b_i(x-X_i) + c_i, \quad (A.2)$$

and

$$S_i''(x) = 6a_i(x-X_i) + 2b_i. \quad (A.3)$$

Now, by setting $S_i(X_i) = Y_i$ and $S_i(X_{i+1}) = Y_{i+1}$, Equation(A.1) yields

$$Y_i = d_i, \quad (A.4)$$

$$Y_{i+1} = a_ih_i^3 + b_ih_i^2 + c_ih_i + d_i, \quad (A.5)$$

where $h_i=X_{i+1} - X_i$.

At each of the interior points, we set

$$S_i'(X_{i+1}) = S_{i+1}'(X_{i+1}),$$

or

$$3a_ih_i^2 + 2b_ih_i + c_i = c_{i+1}, \quad (A.6)$$

and

$$S_i''(X_{i+1}) = S_{i+1}''(X_{i+1}),$$

or

$$6a_ih_i + 2b_i = 2b_{i+1}, \text{ for } i=1,2,\ldots,n-2. \quad (A.7)$$

Since the second derivative is a piecewise linear function of x,

$$S_i''(x) = \lambda_i + \frac{\lambda_{i+1} - \lambda_i}{X_{i+1} - X_i} (x-X_i) \qquad (A.8)$$

where $\lambda_i = S_i''(X_i)$ and $\lambda_{i+1} = S_i''(X_{i+1}) = S_{i+1}''(X_{i+1})$. Thus, comparing Equations (A.3) and (A.8) there results

$$2b_i = \lambda_i, \qquad (A.9)$$

$$6a_i = (\lambda_{i+1}-\lambda_i)/h_i. \qquad (A.10)$$

From Equations (A.4),(A.5),(A.9) and (A.10) the coefficients of the cubic polynomial in the interval $\{X_i,X_{i+1}\}$ can be expressed in terms of Y_i, Y_{i+1} and λ_i, λ_{i+1} as follows:

$$\begin{aligned} a_i &= (\lambda_{i+1}-\lambda_i)/6h_i, \\ b_i &= \lambda_i/2, \\ c_i &= (Y_{i+1}-Y_i)/h_i - (2\lambda_i+\lambda_{i+1})/6, \\ d_i &= Y_i. \end{aligned} \qquad (A.11)$$

Substituting Equation(A.11) into Equation(A.6) and after some algebric manipulation, we obtain the basic equation of Spline technique as follows:

$$\left[\frac{h_i}{2(h_i+h_{i+1})}\right] \lambda_i + \lambda_{i+1} + \left[\frac{h_{i+1}}{2(h_i+h_{i+1})}\right] \lambda_{i+2} = \frac{3}{h_i+h_{i+1}} \left[\frac{Y_{i+2}-Y_{i+1}}{h_{i+1}} - \frac{Y_{i+1}-Y_i}{h_i}\right], \qquad (A.12)$$

for i=1,2,...,n-1,n-2.

APPENDIX B

λ_1 Integral of $<\Delta F_{BB}>$

Let us denote

$$G(\lambda_1,u) = \frac{\lambda_1^2(u)\cos u}{(1+4\tau\cos u)^{1/2}} \left| H(\pi+u,\lambda_1) \right|^2, \tag{B.1}$$

and

$$I = \{\int_{-\pi/2}^{\pi/2} - \int_{\pi/2}^{\pi-u_o} - \int_{\pi+u_o}^{3\pi/2}\} G(\lambda_1,u)du. \tag{B.2}$$

where $\tau=\omega U/g$, $H(\pi+u,\lambda_1)$ and $\lambda_1(u)$ are defined in Equations (3.1) and (3.2), respectively. As shown in Figure 2, λ_1 becomes infinite as u approaches to $\pi/2$, and if λ_1 becomes large, the integrand of Equation(3.1) oscillates so rapidly that it is difficult to evaluate the integral properly. We will examine the second integral of Equation(B.2) first. Let us assume that there exist a small positive angle u_ε such that as $u_\varepsilon \to 0$, we have

$$\int_{\pi/2}^{\pi-u_o} G(\lambda,u)du \simeq \int_{\pi/2+u_\varepsilon}^{\pi-u_o} G(\lambda,u)du, \tag{B.3}$$

where the subscript "i" of λ is omitted for the brevity sake. Let us define the difference between the exact and the approximate value by

$$\text{Error} \equiv \int_{\pi/2}^{\pi/2+u_\varepsilon} G(\lambda,u)\,du, \tag{B.4}$$

and determine the angle u_ε such that the Error is within an acceptable limit. In order to do this, let us examine the magnitude of the Kochin function:

$$H(\pi+u,\lambda) = \int_{-1}^{1} dx\ \exp(i\lambda x\cos u)\int_{C(x)} d1\lambda\psi(n_3+in_2\sin u)$$

$$\times\ \exp\{\lambda(z + iy\sin u)\}\ ,\ \text{for}\ \pi/2\leq u \leq \pi/2+u_\varepsilon. \quad (B.5)$$

Here we neglect the term $(i\omega n)$ in Equation(3.1) under the assumption that λ is very large. Using Equation(3.30) we can approximate the Kochin function for a large value of λ as follows:

$$H(\pi+u,\lambda) \simeq \int_{-1}^{1} dx\ \exp(i\lambda x\cos u)\ \sum_{j=1}^{n-1}\ f_j(x;,\bar{y}_j,\bar{z}_j,u)$$

$$\times \int_{ds_j} ds\ \lambda\exp\{\lambda(z+iy\sin u)\}$$

where $f_j(x;\bar{y}_j,\bar{z}_j,u)= \psi_j(n_{3j}+in_{2j}\sin u)$ and $(\bar{y}_j,\bar{z}_j)$ is the magnitude of the ith segment, and furthermore, considering the fact that $|\exp(i\lambda x\cos u)|$, $|\exp(i\lambda y\sin u)|\leq 1.0$, we may have

$$|H(\pi+u,\lambda)|\leq \left| \int_{-1}^{1} dx \sum_{j=1}^{n-1} f_j(x;\bar{y}_j,\bar{z}_j,u)\int_{z_j}^{z_{j+1}} dz\ \lambda\exp(\lambda z)\right|$$

$$\leq \exp(-\lambda|z|_{min})\ |D(u)| \quad (B.6)$$

where $D(u) = \int_{-1}^{1} dx \sum_{j=1}^{n-1}\ f_j(x;\bar{y}_j,\bar{z}_j,u)$ (B.7)

and $|z|_{min}$ is the minimum value of $|z_{j+1}-z_j|$ of all the cross sections. Combining Equations (B.4) and (B.6), and using the mean-value theorem, we have

$$\text{Error} \leq \int_{\pi/2}^{\pi/2+u_\varepsilon} du\ \frac{\lambda^2(u)\cos u}{(1 + 4\tau\cos u)^{\frac{1}{2}}}\ \exp\{-2\lambda|z|_{min}\}|D(u)|^2$$

$$= |D(\bar{u})|^2 \int_{\pi/2}^{\pi/2+u_\varepsilon} du \frac{\lambda^2(u)\cos u}{(1 + 4\tau\cos u)^{\frac{1}{2}}} \exp\{-2\lambda|z|_{min}\}, \quad (B.8)$$

where $D(u)$ defined in Equation(B.7) is a smooth function of u and $\bar{u}$ is the value between $\pi/2$ and $\pi/2+u_\varepsilon$. By change of variable the integral in Equation(B.8) will become

$$\int_0^{u_\varepsilon} du \frac{\lambda^2(u)(-\sin u)}{(1 - 4\tau\sin u)^{\frac{1}{2}}} \exp\{-2\lambda|z|_{min}\}. \quad (B.9)$$

Assuming u_ε is small and keeping the leading term only, we obtain the following:

$$\int_0^{u_\varepsilon} du \frac{\nu^2}{\tau^4 u^3} \exp\left(-\frac{2\nu}{\tau^2 u^2}|z|_{min}\right) . \quad (B.10)$$

We will denote Equation(B.10) as Δ and again apply the change of variable, $u^2 = v$, the result will be

$$\Delta \equiv \frac{\alpha}{2}\int_0^{u_\varepsilon^2} \frac{\exp(-\beta/v)}{v^2} dv = \alpha/(2\beta)\exp(-\beta/u_\varepsilon^2), \quad (B.11)$$

where $\alpha = \nu^2/\tau^4$ and $\beta = 2\nu|z|_{min}/\tau^2$.

Let us put

$$\alpha/(2\beta)\exp(-\beta/u_\varepsilon^2) \leq 10^{-P}, \quad (B.12)$$

where the arbitrary positive value P will decide the accuracy of computation and the angle u_ε simultaneously. Equation(B.12) can be rewritten as

$$\frac{\alpha}{2\beta}\, 10^{P} \leq \exp(\beta/u_{\varepsilon}^{2}),$$

or

$$\ln\left(\frac{\alpha}{2\beta}\, 10^{P}\right) \leq \beta/u_{\varepsilon}^{2},$$

and if $\frac{\alpha}{2\beta}\, 10^{P} \geq 1.0$, then we will have

$$u_{\varepsilon} \leq \{\beta/\ln(\alpha 10^{P}/(2\beta))\}^{\frac{1}{2}}. \qquad (B.13)$$

This value u_{ε} gives the absolute magnitude of the integral of Equation (B.4), not a relative size of error, i.e., the ratio of the magnitude of Equation(B.4) to that of Equation(B.3). Because of the difficulty of integration of Equation(B.3), we cannot confirm the validity of Equation (B.13) but, in the following example, we show the numerical vlaues of Equation(B.3) for several different P's. In stead of a actual ship, a rectangular barge is considered for an example with the following conditions:

$L/B = 7.5,$
$B/T = 2.0,$
$F_n = 0.2,$
$\beta = 135$ (degree),
$\lambda/L = 2.0,$
$|z|_{min}/B = 0.1.$

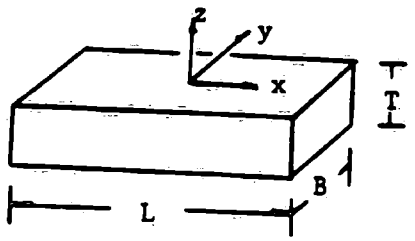

In addition to these the velocity potential ψ in Equation(B.5) is assumed to be constant. The Kochin function $H(\pi+u,\lambda)$ is obtained in the close form, i.e.,

$$H(\pi+u,\lambda) = \frac{4\sin(\lambda l \sin u)}{\lambda \cos u}\left\{\frac{e^{-\lambda}\sin(\lambda \sin u)}{\sin u} - i\sin u\cos(\lambda\cos u)(e^{-\lambda}-1)\right\}$$

where $l=L/2$, and the integral of Equation(B.3) may be summarized as follows:

P	u_ε (degree)	$\lambda(u_\varepsilon)$	$I_P=\int_{\pi/2+u_\varepsilon}^{\pi-u_o} G(\lambda,u)du$	I_P/I_4
3	25.68	4.87	-9043.66	1.0000
4	22.51	6.98	-9073.47	1.0033
5	20.28	9.11	-9114.01	1.0078
6	18.61	11.26	-9144.22	1.0111
7	17.29	13.43	-9169.18	1.0139
8	16.22	16.62	-9187.22	1.0159
9	15.32	17.83	-9211.14	1.0185
10	14.56	20.05	-9225.95	1.0202

where $u_o=\cos^{-1}(1/4\tau)=71.39^o$. Though P increases from 3 to 10, the total increment of Equation(B.3) for P=10 is about 2% of the integration for P=3. The integral does not converge as fast as P grows, but it does approach to finite value as P becomes large.

The third integral of Equation(B.2) is identical to the second one, and because $\lambda(\pi/2-u_\varepsilon) > \lambda(\pi/2+u_\varepsilon)$, the angle u_ε determined in Equation(B.13) can also be used for the first integral of Equation(B.2). Consequently, we have

$$I = \{\int_{-\pi/2+u_\varepsilon}^{\pi/2-u_\varepsilon} - \int_{\pi/2+u_\varepsilon}^{\pi-u_o} - \int_{\pi+u_o}^{3\pi/2-u_\varepsilon}\} G(\lambda,u)du. \qquad (B.14)$$

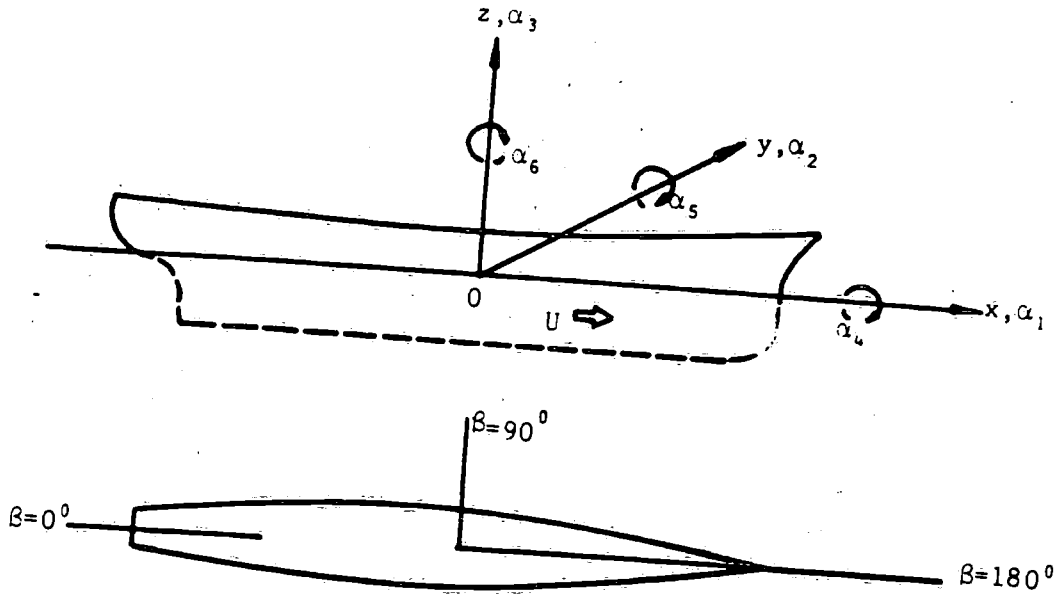

α_1 = surge α_2 = sway α_3 = heave

α_4 = roll α_5 = pitch α_6 = yaw

β = 180^0 head seas
90^0 beam seas
0^0 following seas

Figure 1 - Coordinate System

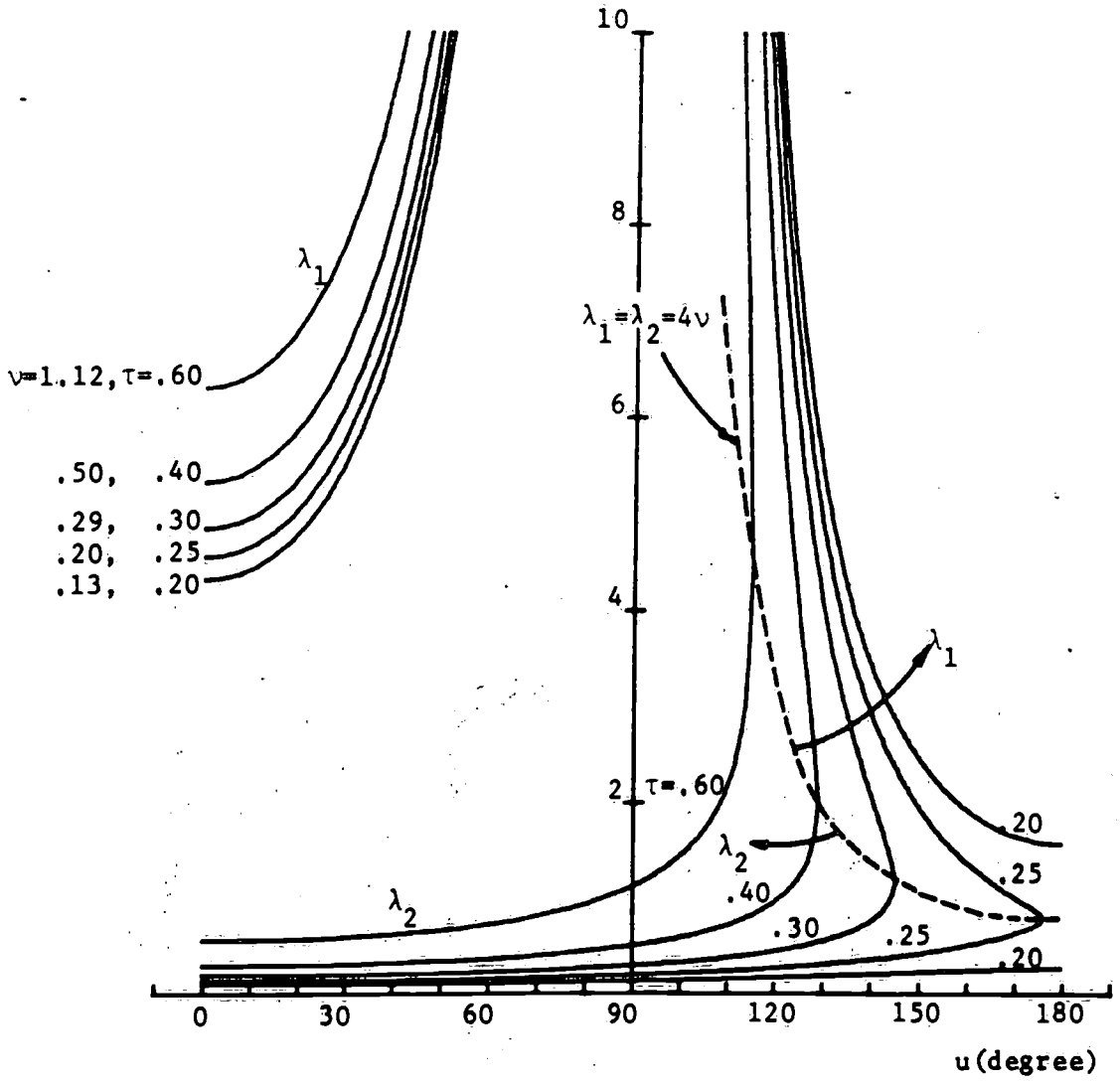

Figure 2 - λ_1 and λ_2 {from Equation(3.2)}

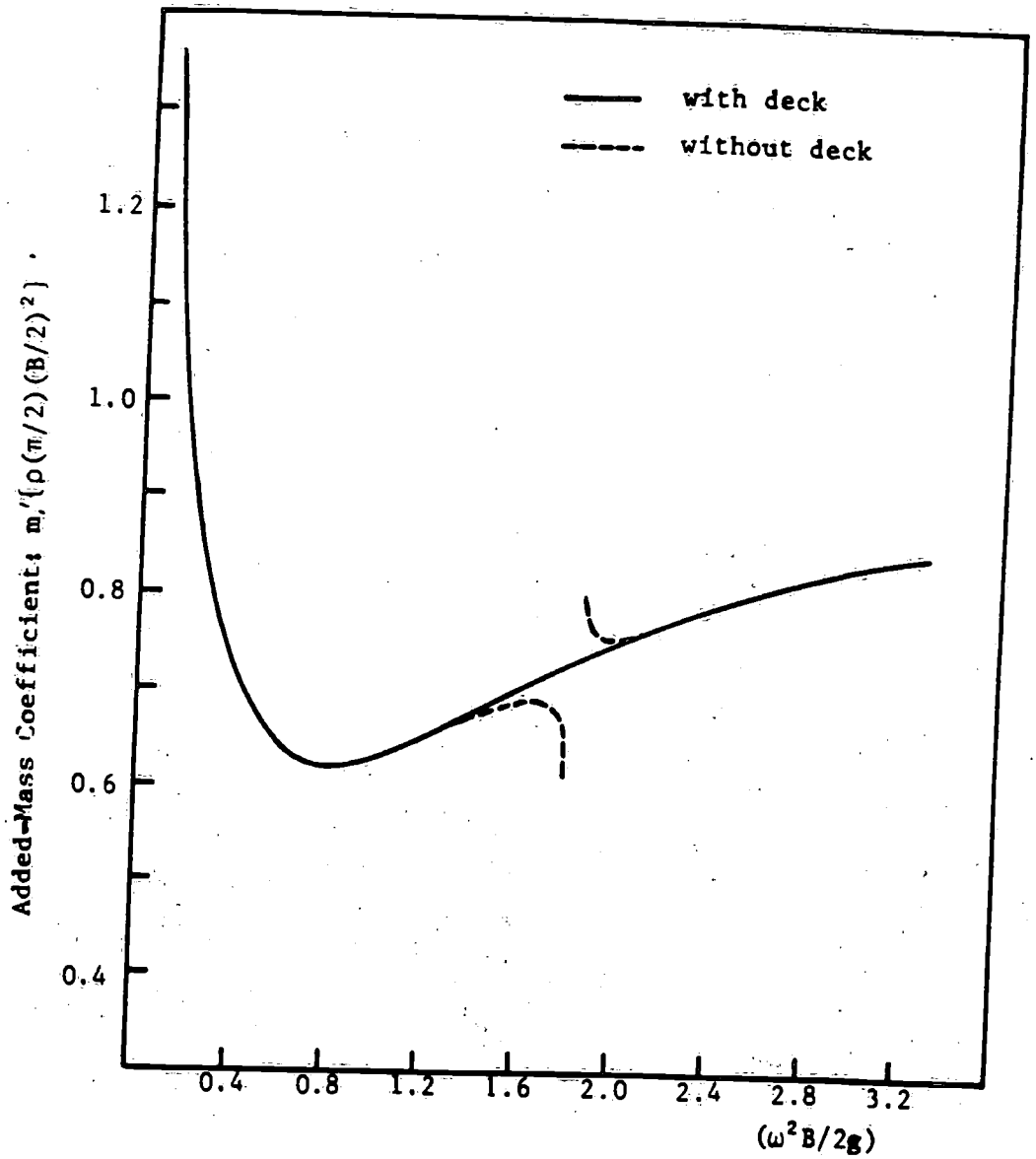

Figure 4 - Heave Added-Mass Coefficients of a Semi-Immersed Circular Cylinder

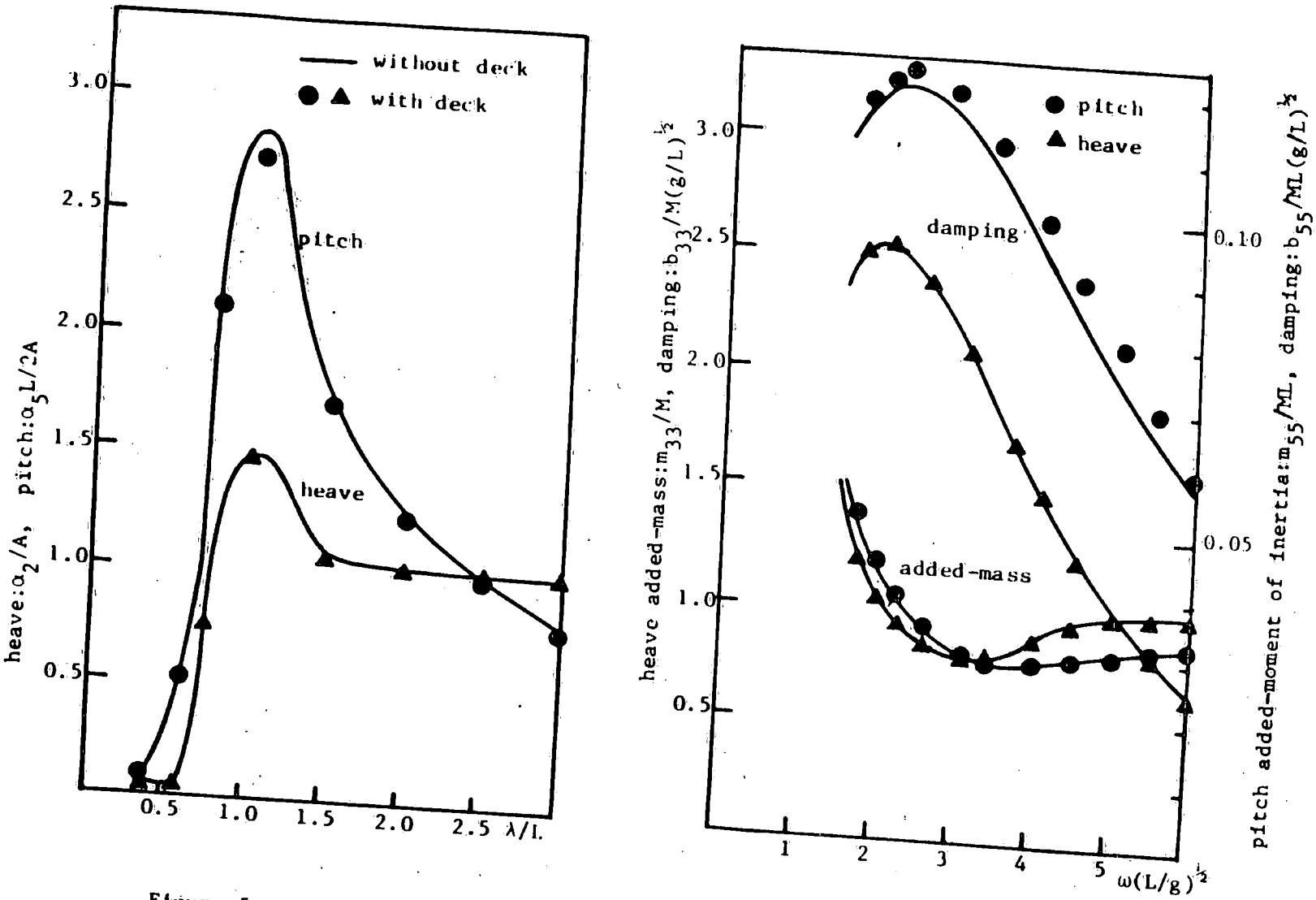

Figure 5 - Added-Mass, Damping Coefficients and Heave, Pitch Amplitude for Mariner at $F_n=0.20$, $\beta=135^0$

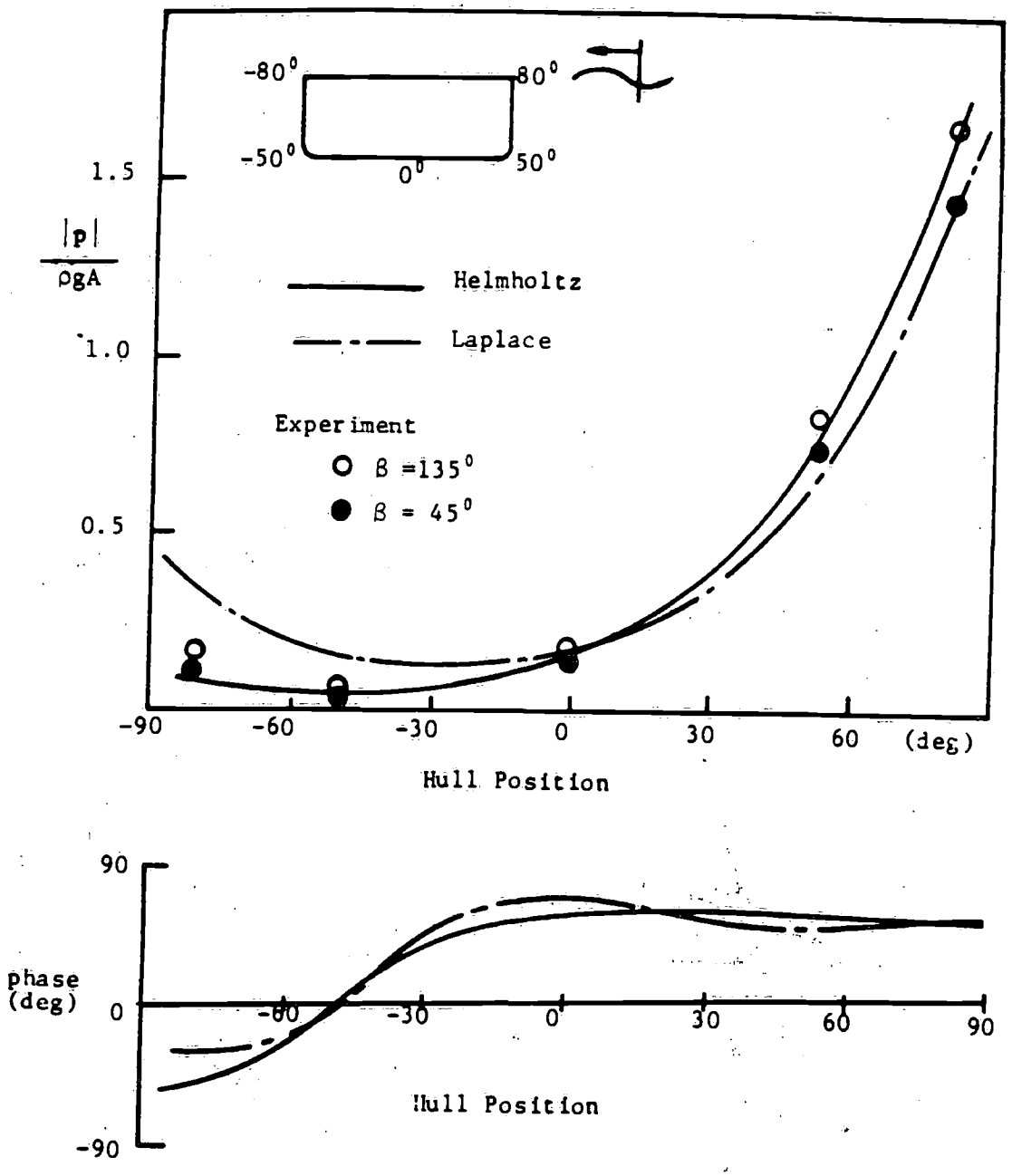

Figure 6 - Girthwise Pressure Distribution for a Midship Section of an Ore Carrier in Oblique Sea {Troesch(1976), Figure 7, p.66}

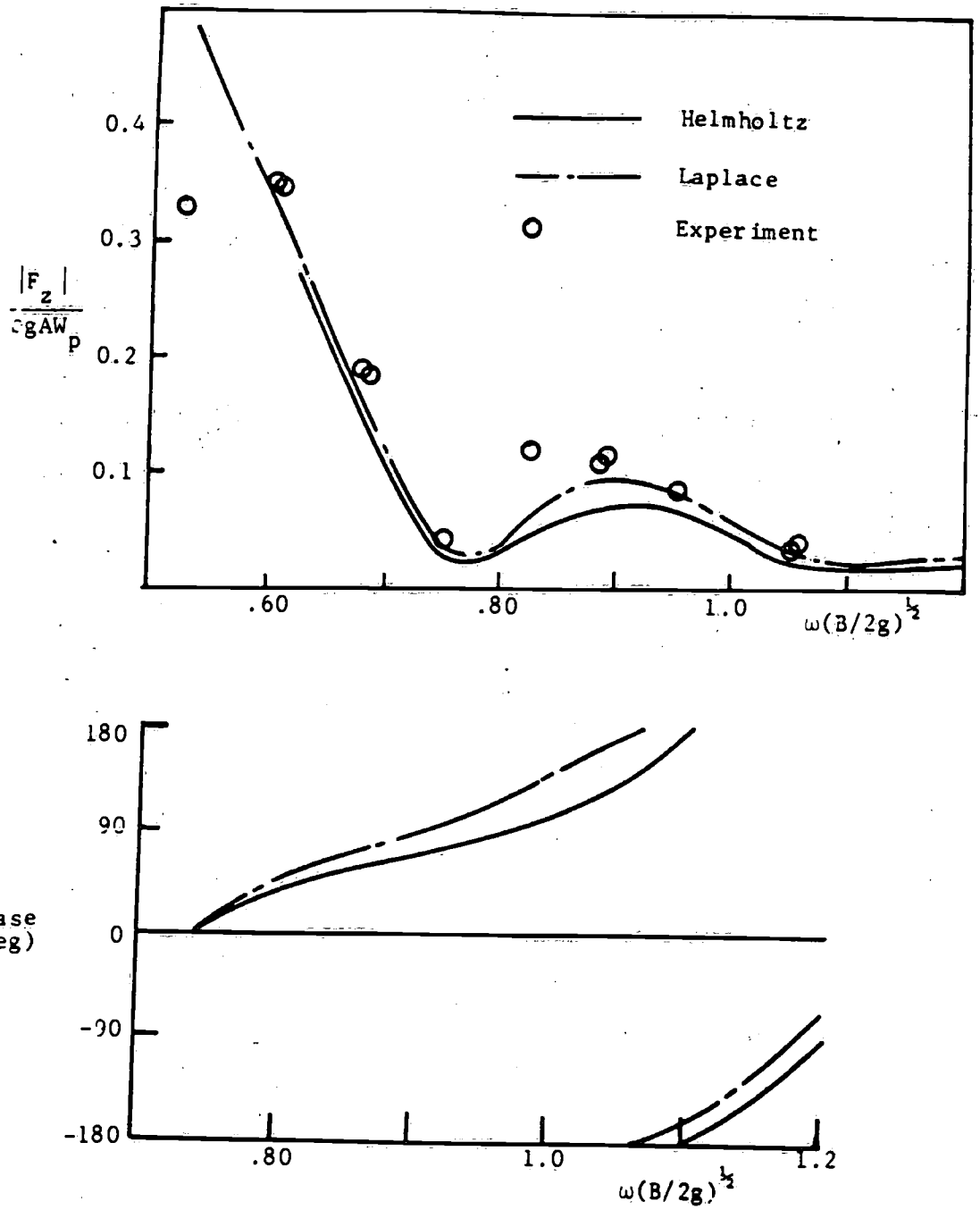

Figure 7 - Total Force for a Series 60, C_B=.70 Hull Form in Oblique Waves (β=30°)
{Troesch(1976), Figure 19, p.84}

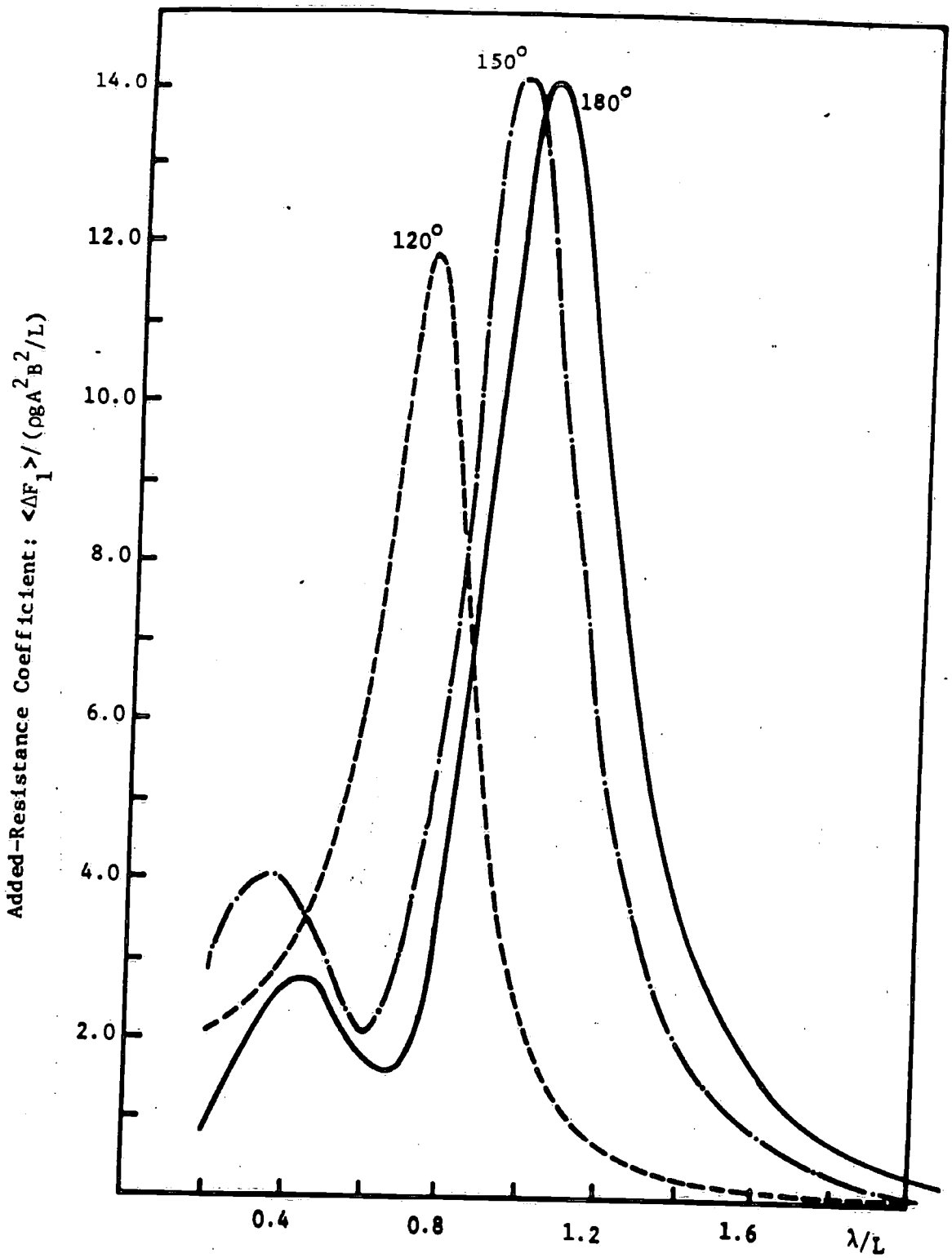

Figure 9 - Added-Resistance Coefficients for Mariner at F_n=0.194

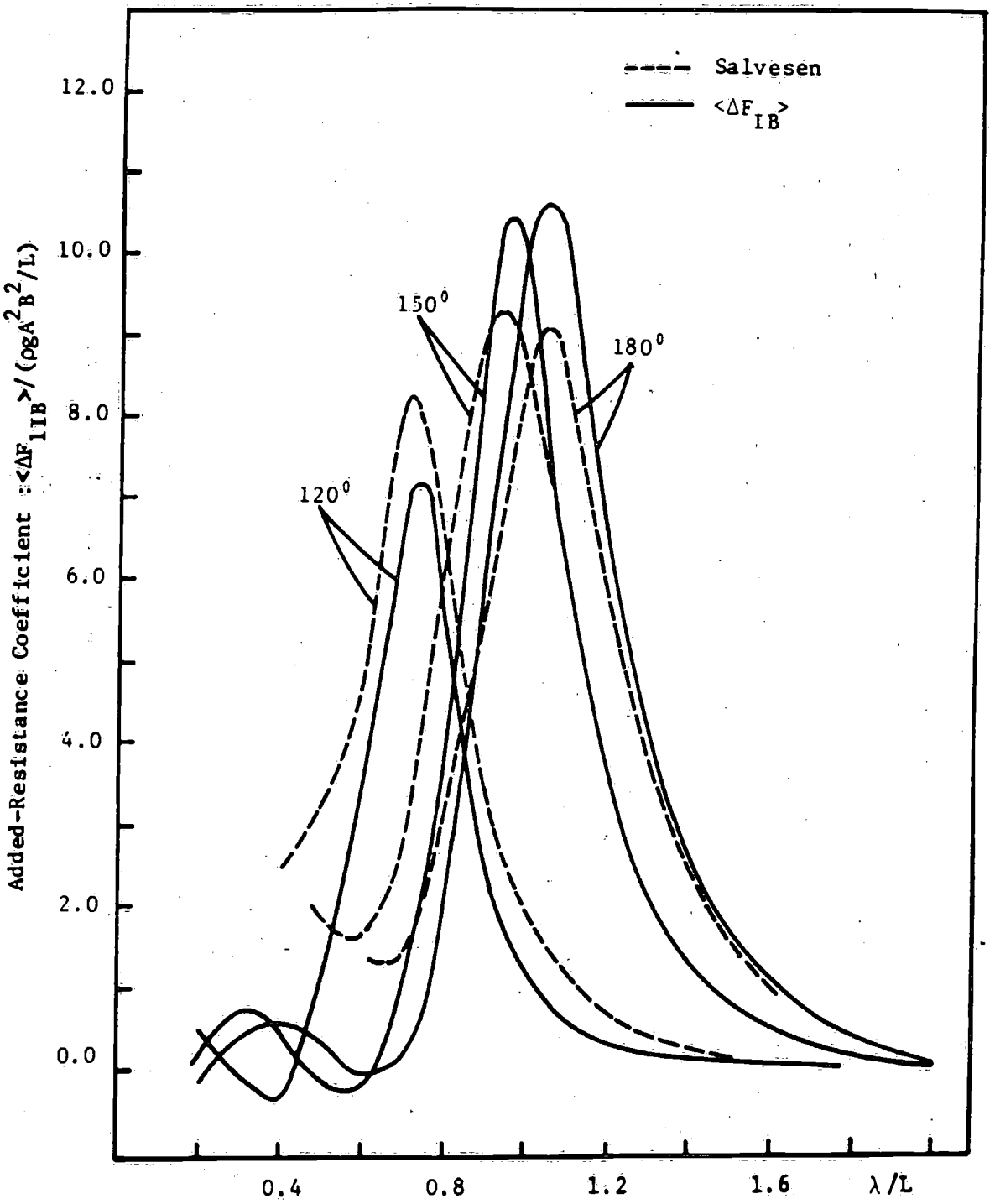

Figure 10 - Comparison between Salvesen and$\langle \Delta F_{1IB} \rangle$ at F_n=0.194

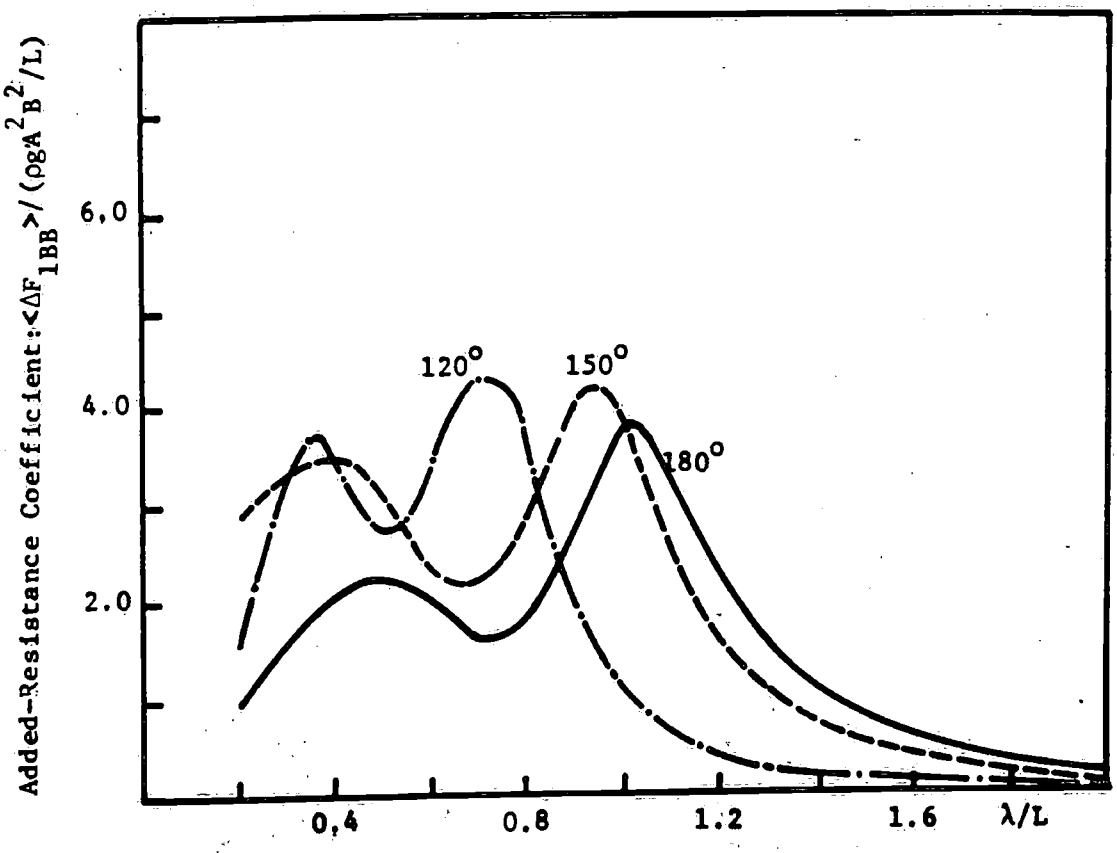

Figure 11 - $\langle \Delta F_{1BB} \rangle$ for Mariner at F_n=0.194

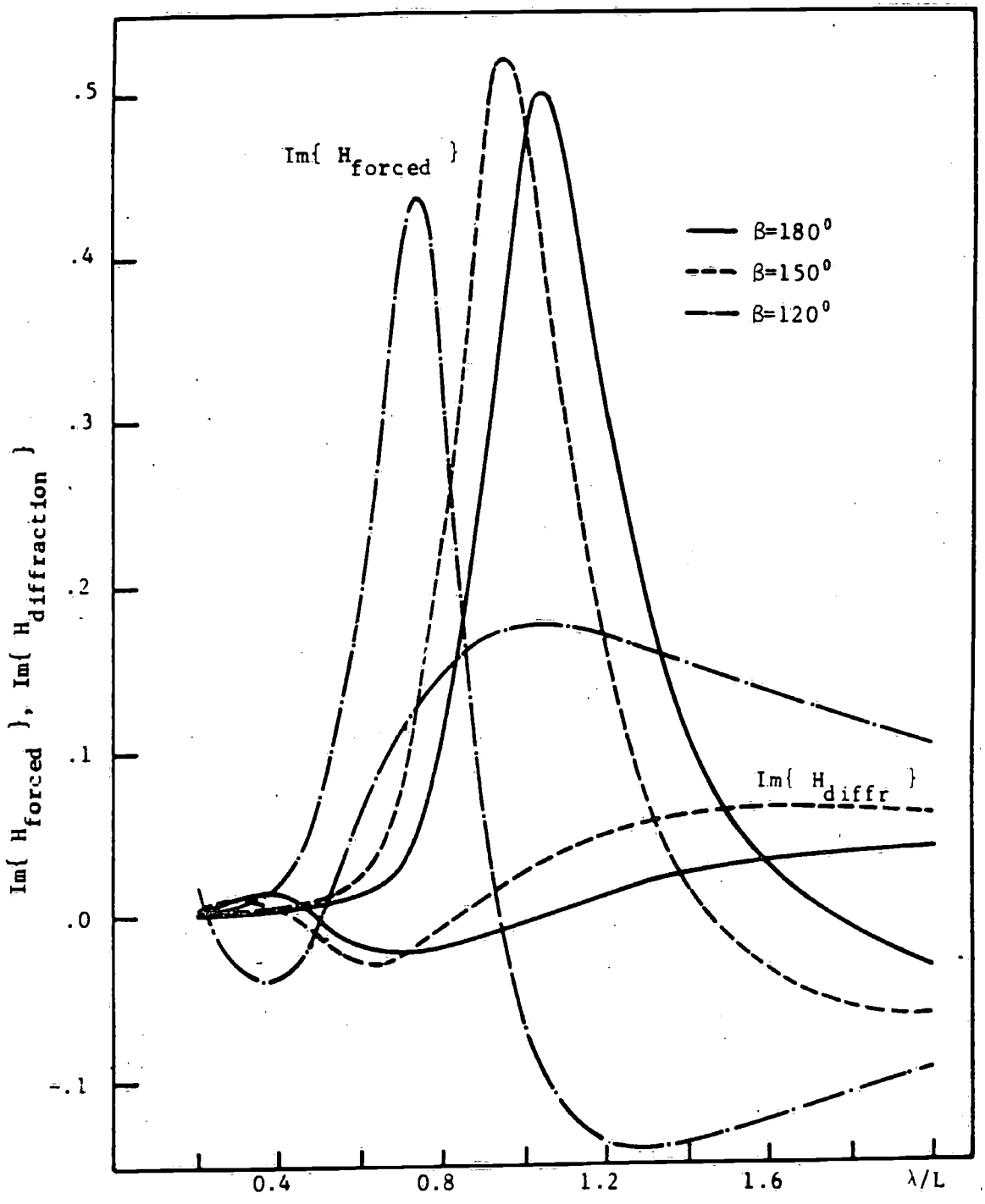

Figure 12 - The Contribution of Forced Motion and Diffraction Part to $\langle \Delta F_{1IB} \rangle$ at F_n=0.194

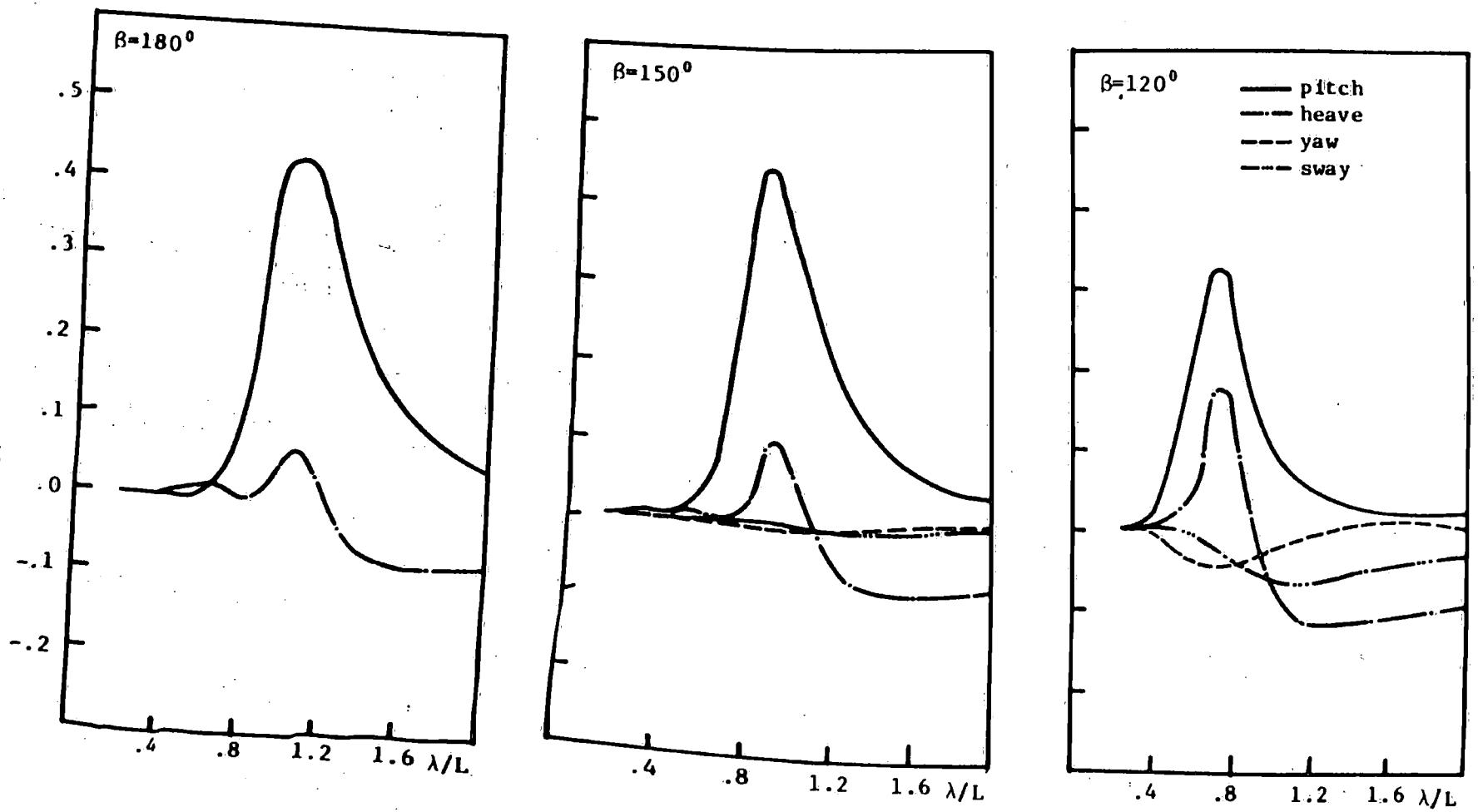

Figure 13 - Relative Magnitude of Each Mode of Ship Motion in $\langle \Delta F_{1IB} \rangle$ at F_n=0.194

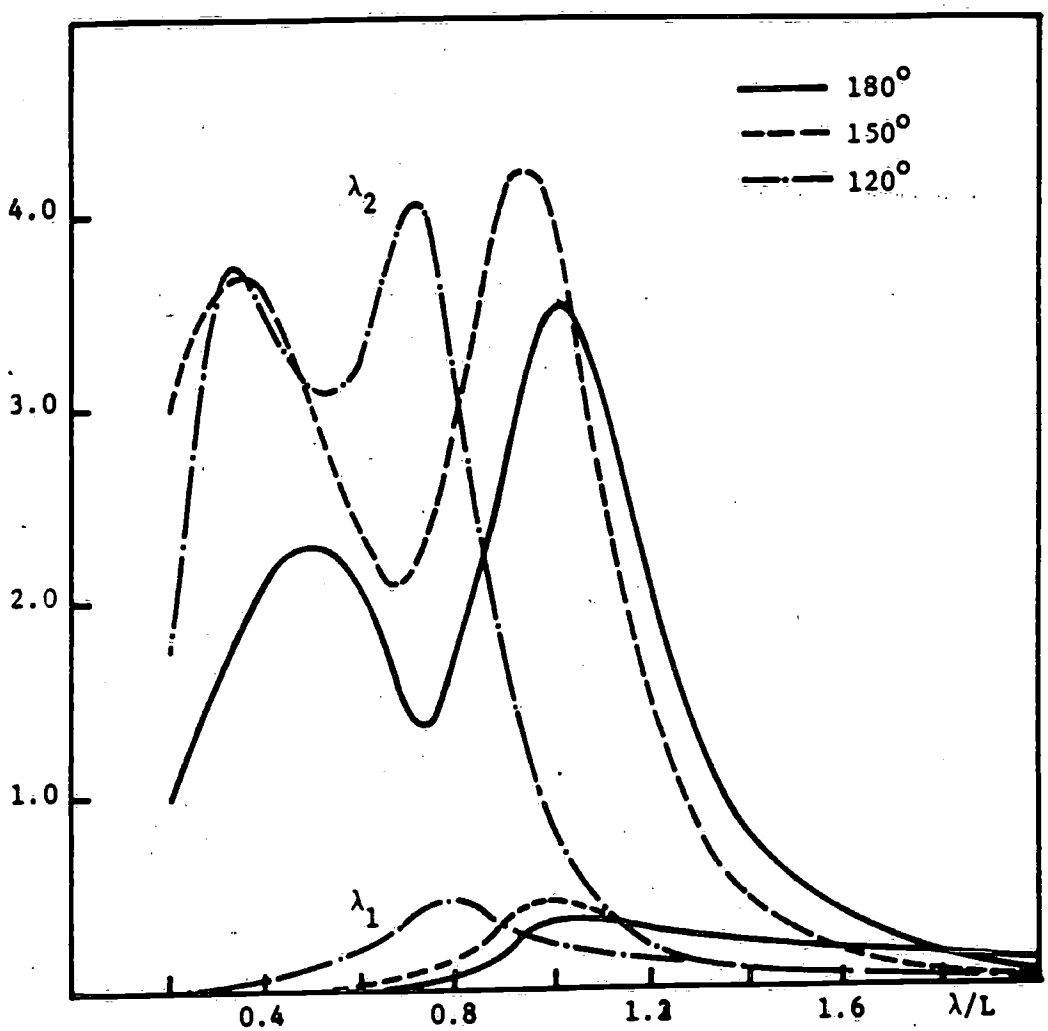

Figure 14 - Comparison between λ_1 and λ_2 Integral of $\langle \Delta F_{1BB} \rangle$ at $F_n = 0.194$

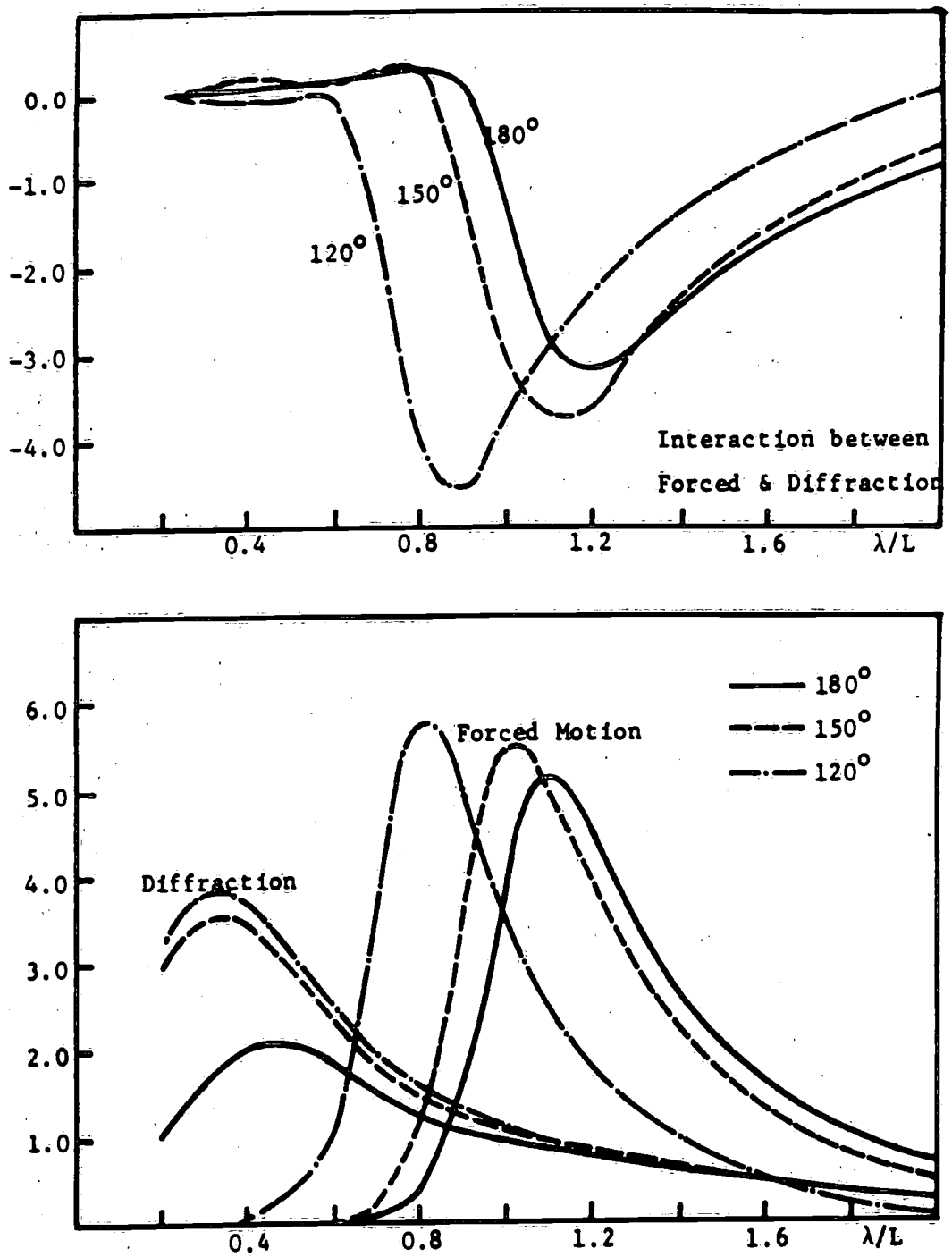

Figure 15 - Forced Motion, Diffraction and Their Interaction of $\langle \Delta F_{1IB} \rangle$ at F_n=0.194

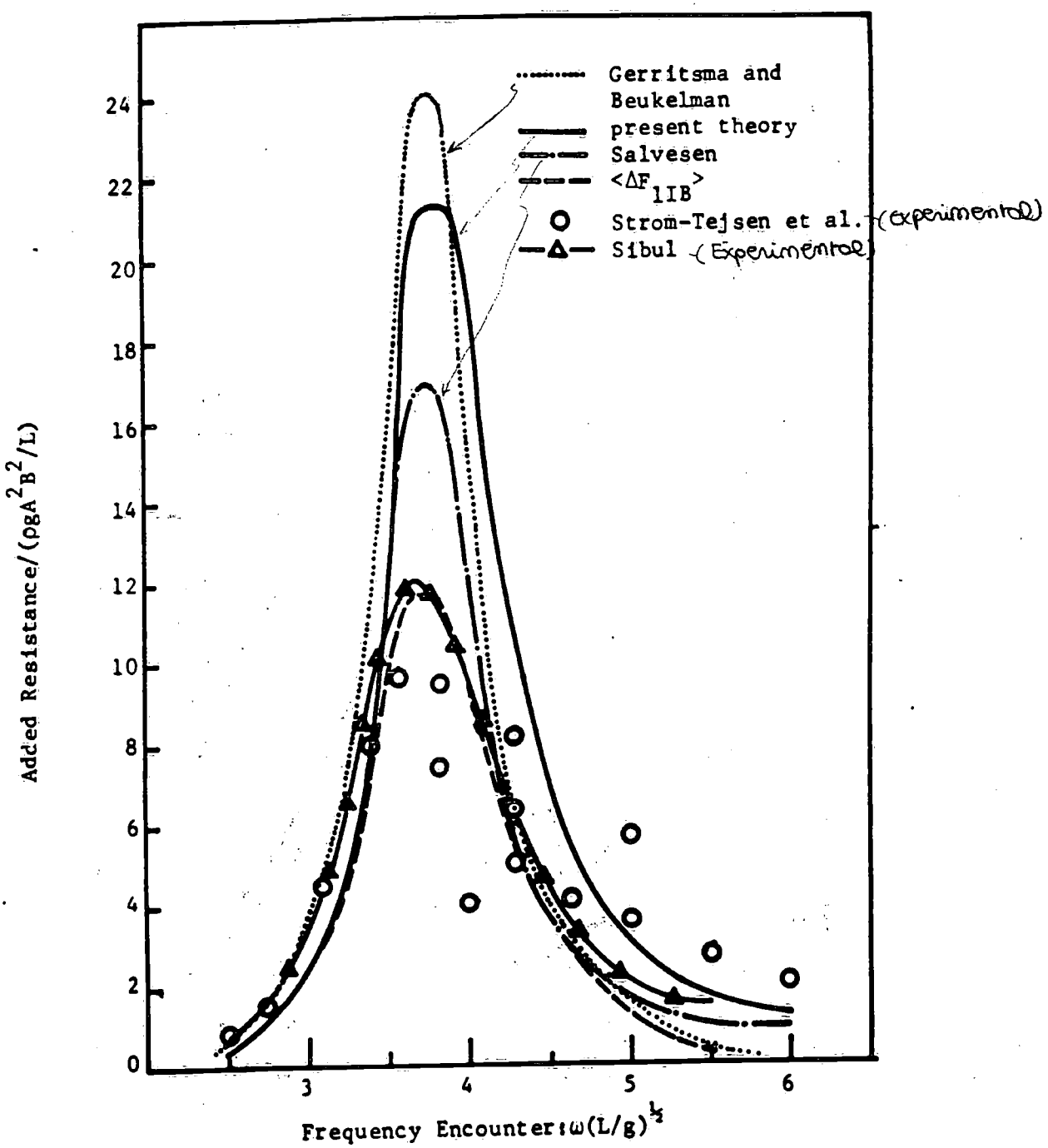

Figure 16 - Comparison of Experimental and Theoretical Added Resistance for Series 60 Hull with C_B=0.60 at F_n=0.283, β=180° [Head Seas]

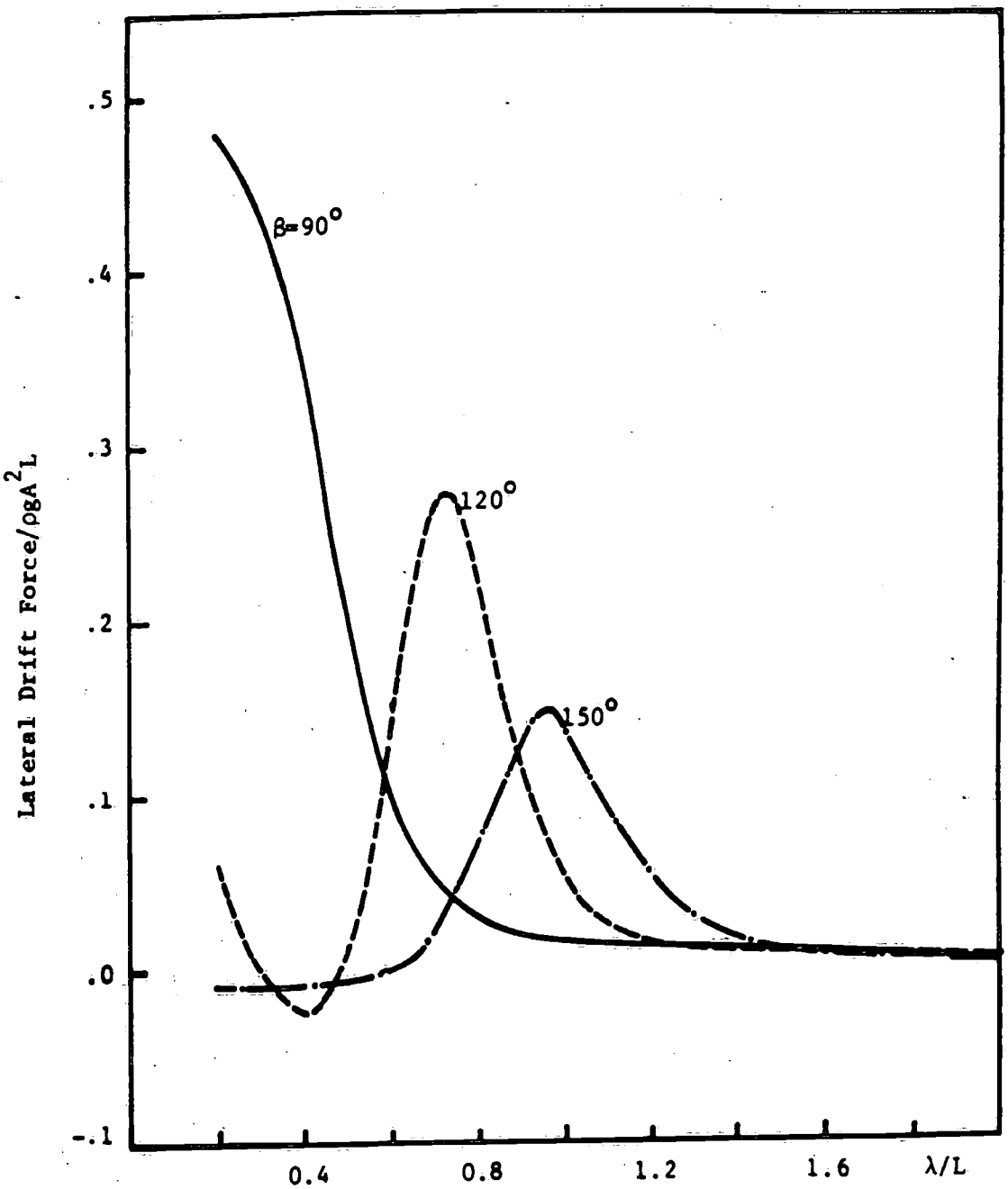

Figure 17 - Lateral Drift Force, $\langle \Delta F_2 \rangle$, for Mariner at F_n=0.194

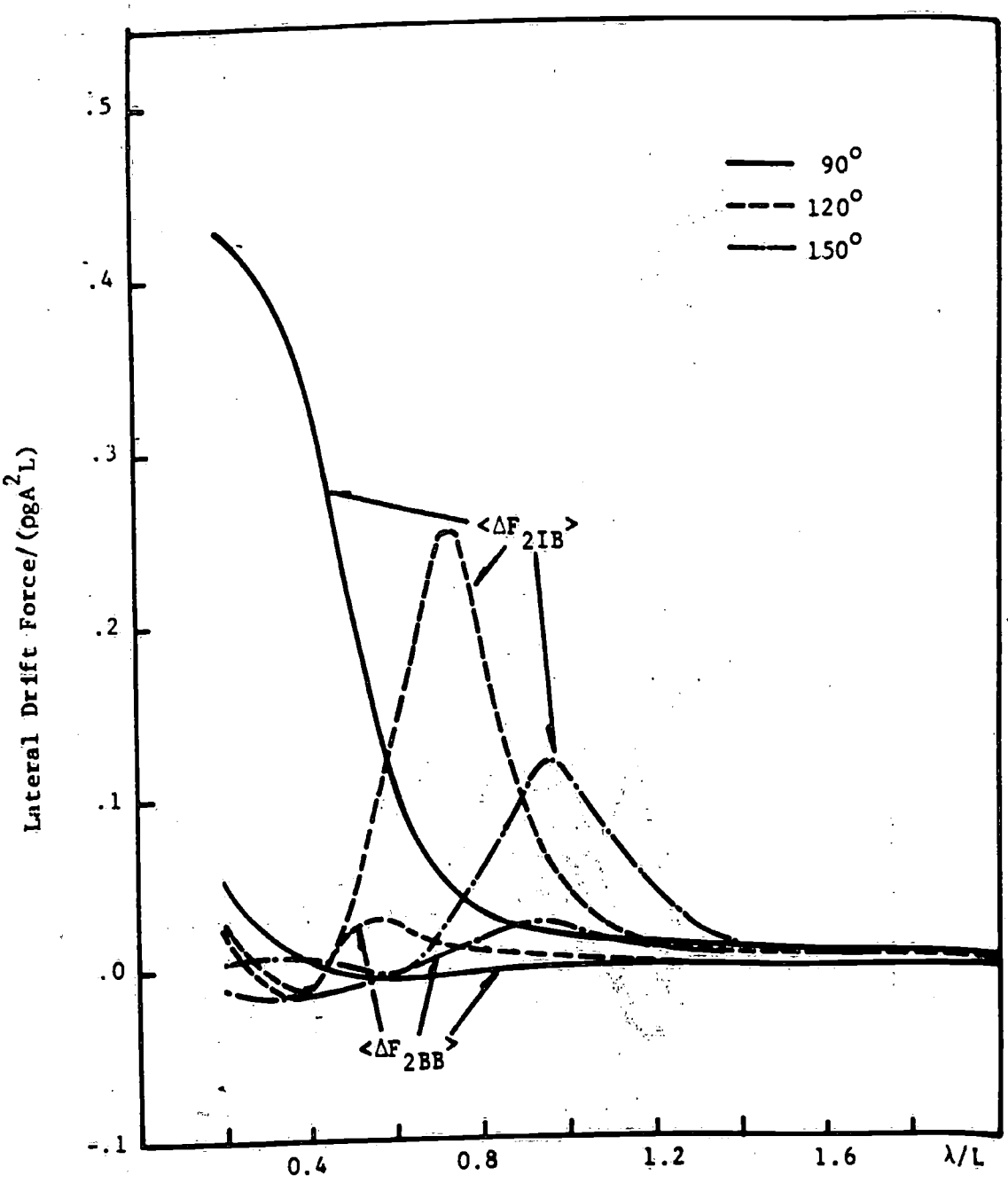

Figure 18 - Relative Magnitude of $\langle \Delta F_{2IB} \rangle$ and $\langle \Delta F_{2BB} \rangle$ for Mariner at $F_n = .194$